

---

# Planetary rings and other astrophysical disks

H. N. LATTER, G. I. OGILVIE, H. REIN

## Abstract

This chapter explores the physics shared by planetary rings and the various disks that populate the Universe. It begins with an observational overview, ranging from protoplanetary disks to spiral galaxies, and then compares and contrasts these astrophysical disks with the rings of the Solar System. Emphasis is placed on fundamental physics and dynamics, and how research into the two classes of object connects. Topics covered include disk formation, accretion, collisional processes, waves, instabilities, and satellite-disk interactions.

## 1.1 INTRODUCTION

Disks are ubiquitous in astrophysics and participate in some of its most important processes. Most, but not all, feed a central mass: by facilitating the transfer of angular momentum, they permit the accretion of material that would otherwise remain in orbit (Lynden-Bell and Pringle, 1974). As a consequence, disks are essential to star, planet, and satellite formation (McKee and Ostriker, 2007; Williams and Cieza, 2011; Papaloizou and Terquem, 2006; Peale, 1999). They also regulate the growth of supermassive black holes and thus indirectly influence galactic structure and the intra-cluster medium (Volonteri, 2010; Fabian, 2012). Although astrophysical disks can vary by ten orders of magnitude in size and differ hugely in composition, all share the same basic dynamics and many physical phenomena. This review explores these areas of overlap.

The prevalence of flattened astrophysical systems is a result of dissipation and rotation (Goldreich and Tremaine, 1982). A cloud of gas or debris in orbit around a central mass conserves its total angular momentum but not its energy, as there are numerous processes that may cool the cloud (inelastic physical collisions, Bremsstrahlung, molecular line emission, etc.). As a result, particles' random velocities are steadily depleted — where 'random velocity' is understood to be the component surplus to the circular orbit fixed by the angular momentum. The system contracts into a flat circular disk, the lowest energy state accessible. The contraction ends, and an equilibrium balance achieved, once the cooling is met by heating (supplied by external irradiation or an internal viscous stress).

Let us define a cylindrical coordinate system with its origin at the central mass and the vertical pointing in the direc-

tion of the total angular momentum vector. We describe systems as *cold* when the pressure gradient is weak and the final equilibrium very thin: radially the dominant force balance is between the centrifugal force and gravity, while vertically it is between pressure and gravity. Systems described as *hot* have stronger pressure and settle into thick disks or tori. At the far extreme, when rotation is subdominant, spheroidal morphologies ensue: examples include planets, stars, globular clusters, elliptical galaxies, etc.

What determines the importance of pressure, and which state is ultimately achieved, is the relative efficiency of heating and cooling. In dense planetary rings, energetic losses from strongly inelastic collisions predominate. Rings are hence exceptionally cold and thin (Colwell et al., 2009). In comparison, radiative cooling in gaseous disks varies by orders of magnitude, depending on the temperature, dust levels, ionisation fraction, or other properties (e.g. Bell and Lin, 1994; Abramowicz and Fragile, 2013). The heating rate also varies considerably, especially if turbulence or external radiation is present. Consequently, gaseous accretion disks can be thin (though never as thin as dense rings) or so thick they resemble doughnuts more than they do sheets.

This fundamental paradigm accommodates a diversity of different astrophysical disk systems, ranging over an enormous variety of length scales, physical properties, and compositions. In the next section we review the observational literature on these systems. We then make clear their key distinguishing physics and physical scales, extending the schematic account above. The rest of the chapter visits an assortment of topics that provide enlightening comparisons between planetary rings and other astrophysical disks. In particular, we dwell on instances of pollinisation between the two fields of study. The topics covered include: formation, accretion, collisional dynamics, waves, instabilities, and finally satellite–disk interactions. We conclude by speculating on further connections between planetary rings and other disks that future work might explore.

## 1.2 OVERVIEW OF ASTROPHYSICAL DISKS

### 1.2.1 Protoplanetary disks

Since the Copernican revolution astronomers have recognised that the planets of the Solar System all orbit the Sun

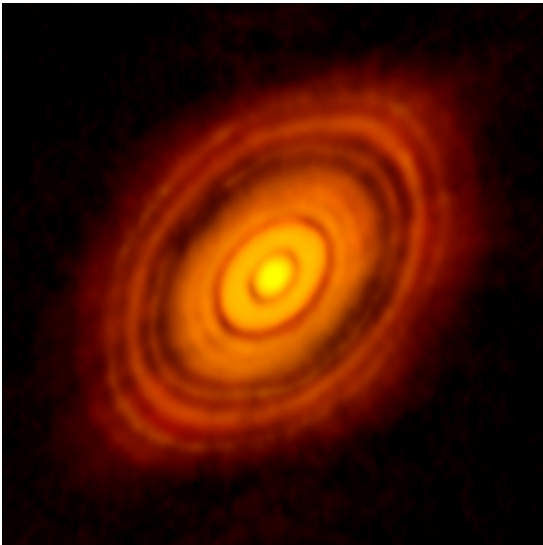


**Figure 1.1** ALMA image of the young star HL Tau and its protoplanetary disk in the mm continuum. Credit: ALMA/ESO

in the same sense, and almost in the same plane. In the eighteenth century Swedenborg, Kant, and Laplace, recognising that this arrangement could not have arisen by chance, proposed that the planets condensed out of a flattened cloud of gas rotating around the Sun earlier in its life (Montmerle et al., 2006, and references therein). Their models of the solar nebula introduced the concept of the protoplanetary disk (hereafter ‘PP disk’) which, though abandoned briefly in the early twentieth century (e.g. Jeans, 1917), lies at the heart of modern theories of star and planet formation.

Originally inferred from the infrared excesses of young stellar objects (e.g. Lada and Wilking, 1984), PP disks were directly imaged first in the sub-mm (Sargent and Beckwith, 1987; Koerner et al., 1993), and then spectacularly in the optical, when the Hubble Space Telescope uncovered a number of examples in the Orion Nebula (McCaughrean and O’Dell, 1996). PP disks consist of relatively cool gas, mostly  $\text{H}_2$ , scattered with dust. Temperatures are  $\sim 100$  K generally, but can reach  $\sim 3000$  K in the inner radii. They are believed to survive for a few million years, extend radially up to  $\sim 1000$  AU, and exhibit aspect ratios of roughly  $H/r \sim 0.05$ , where  $H$  is the disk’s vertical pressure scale-height and  $r$  is radius (Kenyon and Hartmann, 1995; Evans et al., 2009; Williams and Cieza, 2011).

Observations of UV excess in the stellar spectrum allow astronomers to estimate the mass transfer rate through the disk and onto the young star. Comparison of different systems suggests that accretion is irregular, with some 50% of the disk mass falling upon its protostar during less than 10% of the disk’s lifetime (Evans et al., 2009). Archetypal systems that exhibit fast accretion events are the FU Orionis and EX Lupi variables (FUors and EXors), which undergo irregular outbursts of accretion on a range of long timescales, 50–1000 years (Herbig, 1977, 1989; Hartmann and Kenyon, 1996; Audard et al., 2014).

More recent observations using infrared and radio wavelengths (e.g. with Subaru, VLT and ALMA) reveal that PP

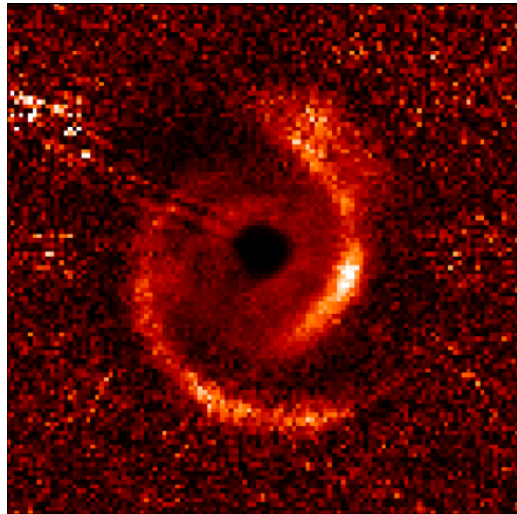


**Figure 1.2** The protoplanetary disk MWC 758 as mapped in polarised scattered infrared with VLT/SPHERE. Credit: Benisty et al. (2015).

disks are highly structured and exhibit gaps, asymmetries, and spirals (Andrews et al., 2011; Muto et al., 2012; Pérez et al., 2014; ALMA Partnership et al., 2015). Figure 1.1 shows an early ALMA image of the disk around HL Tauri, a young Sun-like star, exhibiting a striking array of rings. Figure 1.2 presents a clear example of a spiral density wave in MWC 758. There is considerable research activity aiming to explain the features seen in these and similar images. Embedded planets are the focus of the most popular ideas (e.g. Tamayo et al., 2015), as theory predicts that they naturally carve gaps and excite spiral waves (Papaloizou and Terquem, 2006, see also Section 1.9). However, a panoply of alternatives have been proposed that may bear on the observed structures. These include vortices (Varnière and Tagger, 2006; Lesur and Papaloizou, 2010a), gravitational instabilities (Durisen et al., 2007; Takahashi and Inutsuka, 2014), snow lines (Zhang et al., 2015), stellar flybys (Clarke and Pringle, 1993; Xiang-Gruess, 2016), and warps (Marino et al., 2015a).

### 1.2.2 Dwarf novae, X-ray binaries and Be stars

Most stars form in binary systems. The more massive (primary) star evolves faster than its companion (the secondary) and thus ends up a white dwarf, a neutron star or a black hole while its secondary is left behind on the main sequence. If the binary orbit is sufficiently close, the secondary overflows its critical equipotential surface, or Roche lobe, and spills over towards the compact primary. Owing to its rotation in the binary orbit, the transferred gas has too much angular momentum to fall directly on to the surface of the primary. Instead, it forms an accretion disk around it. Under the action of torques within the disk, the gas gradually loses angular momentum, spirals inwards, and is accreted. As the gas falls deeper into the potential well energy is liberated, and the system becomes luminous (Warner, 1995; Hellier, 2001).

Because such disks possess radii similar to that of the Sun, they are impossible to resolve directly. Instead the above picture of disk formation and accretion was deduced from detailed analyses of spectra and the peculiarities of the systems' light curves, which on the orbital timescale ( $\sim 1$  hour) exhibit characteristic dips and other features (e.g. Kraft, 1962, 1964; Warner and Nather, 1971; Smak, 1971). In Figure 1.3 a representative light curve is presented, showing two key signatures: the eclipse of the compact primary (a white dwarf) and the eclipse of the 'hot spot', the region of the disk struck by the accretion stream from the secondary star.

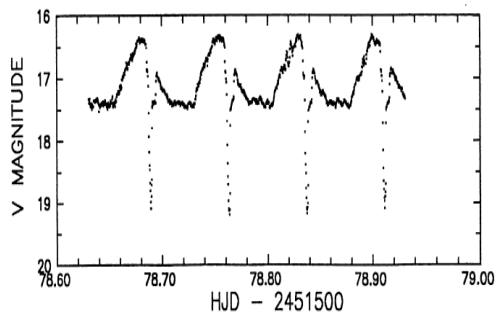


**Figure 1.3** Light curve of the dwarf nova IY UMa over roughly four binary orbits ( $\sim 7$  hours in total). The vertical axis is magnitude in the V band, and the horizontal axis is heliocentric Julian day (HJD). The broad humps correspond to the progress of the hot spot around the disk, while the abrupt dips correspond to eclipses of the white dwarf by the secondary. The points are plotted at 17 s intervals. Credit: Patterson et al. (2000).

Systems with white dwarf primaries are known as cataclysmic variables because many of them exhibit dramatic outbursts. These include the classical novae, in which a layer accreted on the primary ignites in a thermonuclear runaway (Gallagher and Starrfield, 1978; Shara, 1989), and the dwarf novae, in which outbursts occur cyclically and arise from a state change in the disk itself (Warner, 1995; Lasota, 2001). The latter outbursts feature an increase of brightness of some 2–5 magnitudes, last for a few days, and possess a recurrence interval of days to weeks. Figure 1.4 illustrates a clear sequence of dwarf nova outbursts in SS Cygni. Note that some sources exhibit more complicated behaviour such as 'standstills' (*Z Camelopardalis* variables) and 'superoutbursts' (*SU Ursae Majoris* variables) (Warner, 1995).

Systems with neutron star or black hole primaries are known as X-ray binaries because their emission is dominated by high-energy photons. They were first discovered by X-ray satellites launched in the 1960s (Giacconi et al., 1962; Gursky et al., 1966; Sandage et al., 1966). In the following 50 years, space-based X-ray observatories, such as *Einstein*, *Chandra*, and *XMM-Newton*, have uncovered the properties of many such systems, yet because of their weak emission in the optical they are far less well constrained than dwarf novae. Low-mass X-ray binaries, involving low-mass secondaries, typically accrete by Roche-lobe overflow as described above. In contrast, the accretion disks in high-mass X-ray binaries typically capture their gas from the vigorous winds

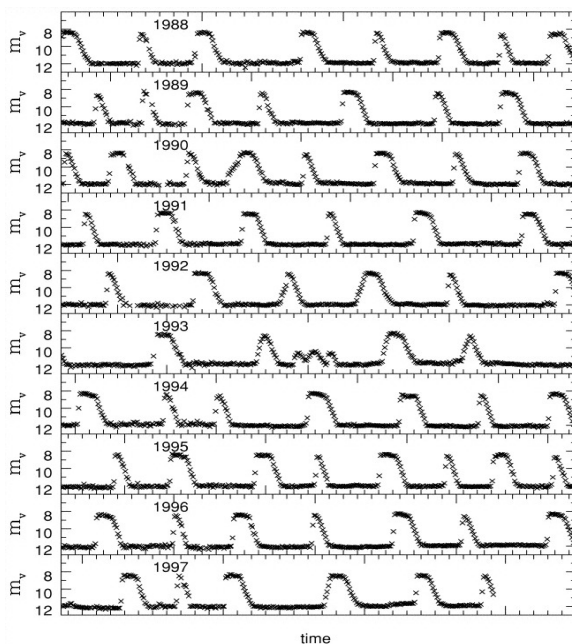


**Figure 1.4** Light curve of SS Cygni on long timescales, showing quasi-periodic outburst behaviour. Each panel represents one year, each small tic on the horizontal axis 10 days, and each cross the daily mean in magnitude — thus small and fine-scale variations (such as in Fig. 1.3) are removed. The first panel begins at HJD 2,446,432, and the last panel ends at 2,450,082. Credit: Cannizzo and Mattei (1998).

of the high-mass secondary stars (Charles and Coe, 2006; Tauris and van den Heuvel, 2006). In both cases the disk temperature is strongly affected by X-ray irradiation and, as a result, though they undergo outbursts, their dynamics can differ markedly from dwarf novae (Lasota, 2001; King, 2006).

The disks associated with interacting binaries usually consist of hydrogen and helium in atomic or ionised form. Dwarf nova disks are vertically thin ( $H/r \sim 0.01$ ), but the aspect ratio varies between the low and the high (outbursting) states, which are characterised by temperatures between  $\sim 3000$  K and  $\sim 50,000$  K at the midplane, respectively (Hellier, 2001). In the inner regions of X-ray binaries the disk attains enormous temperatures, greater than  $10^6$  K at the disk surface, and cycles through a number of poorly understood spectral states, some of which are accompanied by jets of material launched perpendicular to the disk (Remillard and McClintock, 2006; Done et al., 2007).

Finally, we touch on Be stars. These are rapidly spinning B stars in which material is periodically expelled from the equator and forms a centrifugally supported disk. Usually the disks are inferred observationally by their characteristic Balmer lines and their polarisation of the star's continuum radiation (Rivinius et al., 2013), though in the case of  $\zeta$  Tauri, a map of the disk itself has been directly reconstructed using interferometry in the  $H\alpha$  line (Quirrenbach et al., 1994), while peculiarities in the light curves of the eclipsing binaries  $\epsilon$  Aurigae and EE Cephei are best explained by a tilted disk around a B star (Hoard et al.,

2010; Gałan et al., 2012). The mechanism by which material is ejected from the star (the ‘Be phenomenon’) is still debated, but may involve non-radial stellar pulsations, magnetic fields, or winds. Once formed, the disk evolves viscously, while undergoing global eccentric oscillations of unknown provenance (Okazaki, 1991).

### 1.2.3 Debris disks

Debris disks consist of dust and larger solids usually orbiting a young or main-sequence star (Wyatt, 2008). They are the end-points of protoplanetary disk evolution, the gas either accreted or swept away by a photoevaporative wind. Alternatively, they may be regarded as the ‘leftovers’ of the planet formation process (Alexander et al., 2006; Wyatt et al., 2015).

The first debris disk was discovered orbiting Vega by the *IRAS* satellite, its presence betrayed by a large infrared excess (Aumann et al., 1984). Thanks to recent surveys by *Spitzer* and *Herschel*, there are now several hundred debris disk candidates circling a wide variety of stars (Su et al., 2006; Eiroa et al., 2013). Debris disks have also been observed in sub-mm to optical wavelengths and may now be imaged directly, giving astronomers information about their morphology (Wyatt, 2008). These disks are believed to be extrasolar analogues of the asteroid belt, Kuiper belt, and exozodiacal dust in our own Solar System, and so the study of debris disks straddles the two fields of planetary science and astrophysics.

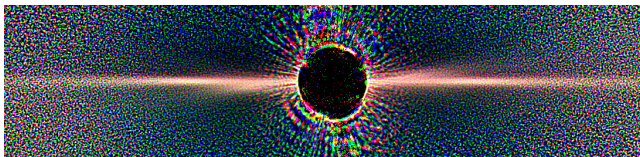


**Figure 1.5** This image shows the edge-on disk around Beta Pictoris, taken by the Hubble Space Telescope. One can identify a primary disk and a secondary, slightly tilted, disk. Credit: ESA/Hubble.

The majority of observed debris disk dust lies in the 1–100  $\mu\text{m}$  size range, and hence their infrared emission is difficult to study from the ground. Typically, the total mass in these grains is significantly less than that of the Earth (Wyatt, 2003, 2008), and is distributed between radii 10–100 AU. Rather than being primordial, the dust must be constantly replenished or else it would be eliminated by radiation pressure, collisional fragmentation, or stellar wind drag. Infrequent impacts between larger bodies are thought to initiate a collisional cascade that supplies this material (Backman and Paresce, 1993; Wyatt and Dent, 2002). Unfortunately, the population of large solids is difficult to observe, owing to their smaller total surface area. Planetary sized objects, however, have been directly imaged and also inferred from perturbations in the dust (see below).

In comparison, we know of several hundred bodies with a size of roughly 100 km in the Kuiper belt, and have constrained some of their surface properties (Petit et al., 2008; Stansberry et al., 2008). Moreover, to explain the frequency

of short-period comets, theoretical estimates show that the belt must contain at least  $10^8$  bodies with sizes greater than 1 km (Farinella and Davis, 1996; Jewitt and Luu, 2000). These estimates provide data on intermediate size bodies in one debris disk, at least.

Direct imaging reveals that debris disks exhibit a range of intriguing morphologies: sharp edges, gaps, warps, rings, spirals, asymmetries, and clumps (Wyatt, 2008). Figure 1.5 shows one of the nearest debris disks, around the star Beta Pictoris. One can identify two disks slightly tilted with respect to each other. Planets can potentially sculpt and structure debris disks (e.g. Mouillet et al., 1997; Wyatt, 2005a; Quillen, 2006; Su et al., 2009), and indeed the tilt evident in Figure 1.5 is thought to be forced by a massive Jovian planet (Lagrange et al., 2009).

### 1.2.4 Active galactic nuclei

It is generally accepted that most galaxies contain a supermassive black hole, of up to a few billion solar masses, at their centres (Ferrarese and Ford, 2005; Merritt, 2013). A small proportion of these are ‘active’, in that they produce immense and persistent volumes of radiation, sometimes orders of magnitude greater than the total power output of their host galaxies. The origin of this spectacular luminosity is the accretion of matter, through which gravitational energy is converted into mechanical and electromagnetic energy. Because of the intense gravity of supermassive black holes, accretion of only one solar mass per year is required to generate the observed luminosities (Salpeter, 1964; Lynden-Bell, 1969; Marconi et al., 2004).

The spectrum of these ‘active galactic nuclei’ (AGN) is strikingly broad, and can extend from the far infrared to hard X-rays; for example, the well studied case of NGC 4151 emits roughly the same specific intensity over five orders of magnitude in frequency (Ulrich, 2000). The optical to extreme ultraviolet light emerges from the accretion disk surrounding the black hole, while the X-rays are generated by the disk’s hot corona of dilute gas. Dust in the disk, or in the systems’ enveloping torus, is responsible for the infrared (Ferrarese and Ford, 2005). The optical and UV emission tells us that the disk surface is no hotter than about  $10^5$  K, though temperatures at the midplane near the black hole can greatly exceed that. Variability on short timescales suggests that disk sizes are typically 1000 AU or less (e.g. Greenstein and Schmidt, 1964; Peterson, 2001). In addition, AGN exhibit strong and broad spectral lines: their large redshifts reveal their distance from our galaxy, while their Doppler-broadened linewidths can constrain the mass of the central black hole, as in the case of M87 (Macchetto et al., 1997). Finally, a subclass of AGN is characterised by powerful radio emission (e.g. Baade and Minkowski, 1954; Fanaroff and Riley, 1974; Miley and De Breuck, 2008), usually accompanied by non-thermal gamma rays (Hartman et al., 1999). This radiation issues from intense relativistic jets oriented perpendicular to the disk plane (e.g. Biretta et al., 1999). Figure 1.6 shows a radio image of such a jet emerging from Cygnus A.

Owing to this collection of varied and unusual properties, several decades passed before AGN were properly identified and understood. In fact, for some time they were classified as separate and distinct sources: Seyfert galaxies, radio galaxies, BL Lac objects, quasars, and blazars. By the early 1980s it was becoming clearer that these classes were different ‘faces’ of the same astrophysical object, an accreting supermassive black hole, with the variation in their observed properties attributed mainly to differing viewing angles, and the presence, or not, of a jet (Rees, 1984; Antonucci, 1993). See Netzer (2015) for a recent discussion of AGN ‘unification’ theories.

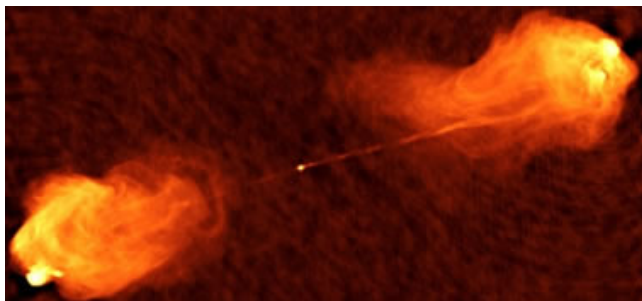


**Figure 1.6** A radio map of the galaxy Cygnus A (at a wavelength of 6 cm). The two jets can be seen emerging from the nucleus of the galaxy and colliding with the intergalactic medium in the two large radio lobes, each roughly 100 kpc from the AGN. Credit: NRAO/AUI.

AGN are of immense importance in galactic astronomy and cosmology. They impact on the structure and evolution of their host galaxies, clearly demonstrated by the strong correlation between an AGN’s mass and the velocity dispersion of its host galaxy’s stars, on one hand, and on the size of the galactic central bulge, on the other (Kormendy and Richstone, 1995; McConnell et al., 2011). They control, to some extent, the dynamics of the intracluster medium of galaxies, via the deposition of mechanical energy through jets (‘AGN feedback’), a process that bears directly on the cooling-flow problem in such systems (Fabian, 2012). AGN emission may also act as a probe of the intervening gas between our galaxy and high redshifts (e.g. Fan et al., 2006). At the same time they pose a number of challenging problems: how do the black holes grow so large? How are relativistic jets launched, and why do only some AGN produce them? Why are they more numerous at large redshift, and does this mean that AGN represent a transient phase of galactic evolution?

### 1.2.5 Tidal disruption events

Spectroscopic evidence indicates that some 20% of white dwarf photospheres are polluted with metal elements (the ‘DAZ phenomenon’, Zuckerman et al., 2003). Moreover, these stars must be continually accreting new pollutants because of the short sinking time of some observed ions (e.g. Mg II) (Holberg et al., 1997; Koester et al., 1997). An additional clue is that a fraction of the most contaminated examples display evidence of a circumstellar dust ring from either

infrared excess (e.g. Farihi et al., 2009) or double-peaked optical emission lines (Gänsicke et al., 2006). As a result, astronomers have deduced that DAZ white dwarfs are ringed by narrow accretion disks of debris and gas, probably the result of the tidal disruption of an asteroid or minor planet (Graham et al., 1990; Debes and Sigurdsson, 2002; Jura, 2003, 2008).

One problem this scenario must overcome is how to supply the white dwarf with a suitable body to disrupt. Asteroid belts and/or planets on wide orbits can survive the giant-branch precursor to the white dwarf (Villaver and Livio, 2007; Bonsor and Wyatt, 2010), but their orbits must be subsequently perturbed so that they plunge to sufficiently small radii. Scattering of asteroids by planets is the currently favoured model, the planetary system wrought dynamically unstable in the post-stellar mass-loss stage (Bonsor et al., 2011; Debes et al., 2012). The intense interest driving this field centres on the make-up of the pollution itself, because it provides an opportunity to directly sample the compositions of rocky exoplanetary systems (e.g. Klein et al., 2010; Gänsicke et al., 2012; Xu et al., 2014).

Similarly, when stars stray too near supermassive black holes they are tidally ripped apart. At early times the stellar material falls on the black hole at a tremendous rate, resulting in a flare whose luminosity approaches that of a supernova. After this initial period ( $\sim 10$  days), the remaining stellar mass accretes via a narrow disk over the course of a few years, the emission at this stage peaking in the UV and soft X-rays (Rees, 1988; Strubbe and Quataert, 2009). First hypothesised in the 1970s (Hills, 1975), such tidal disruption events were not observed until the *ROSAT* All-Sky survey 20 years later (see Komossa and Bade, 1999; Donley et al., 2002). A dozen candidates have been revealed since, some accompanied by short-lived relativistic jets (Bloom et al., 2011; Burrows et al., 2011).

The astrophysical interest in these impressive events lies in their ability to identify and characterise *quiescent* supermassive black holes, which would otherwise lie undetected at the centres of galaxies. They can help astronomers determine black hole spin and study jet launching and accretion disk physics; they may also provide an electromagnetic counterpart to the gravitational waves emitted during the initial accretion of the star (e.g. Kobayashi et al., 2004; Kesden, 2012).

### 1.2.6 Galactic disks

It was Kant, again, who first proposed that the Milky Way was a system of stars orbiting collectively in much the same way as the Solar System. Moreover, he speculated that observed nebulae might be distant ‘island universes’, as vast as the Milky Way. This hypothesis was partly verified by Lord Rosse in 1845, who resolved M51, and a number of other sources, into spiral patterns (Binney and Merrifield, 1998). But it was not till Hubble’s observations of Cepheid variable stars in M33 that it was firmly established that the nebulae were in fact (far) outside the Milky Way and were indeed independent ‘island’ galaxies (Hubble, 1925).



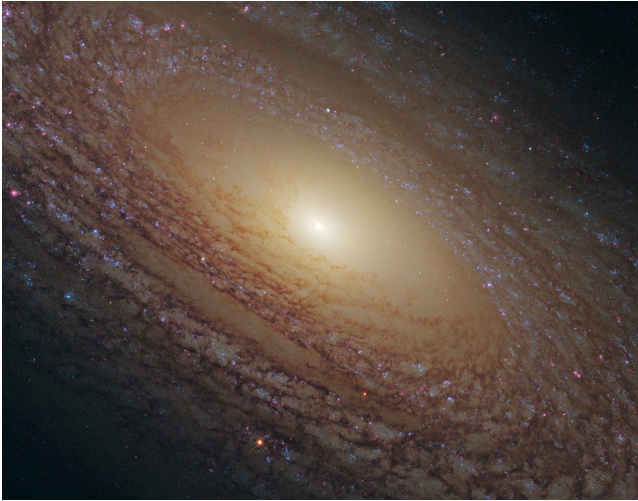


**Figure 1.7** An HST image of the flocculent spiral galaxy NGC 2841. Credit: ESA/HST.

Disk galaxies are flattened structures composed of stars, gas, and dust undergoing, for the most part, rotational motion around the galactic nucleus. Originally classified by Hubble (1936) as part of the Hubble sequence, they differ from most astrophysical disks in that their orbital motion is not entirely dominated by the central object (a supermassive black hole); their rotation curves hence depart significantly from Keplerian. Aside from the initial stage of galaxy formation, there is no accretion throughout the whole disk, per se, mainly on account of there being insufficient rotation periods during a galactic lifetime. Most stars are clearly luminous in the optical and UV; the gas, on the other hand, falls into a variety of thermodynamic phases that emit in correspondingly diverse frequency bands (Field, 1965; McKee and Ostriker, 1977; Draine, 2011).

Galactic disks manifest large-scale features such as spiral arms, central bars, rings, and streams. They also generally possess a central spheroidal bulge, containing older stars, and a large spherical dark matter halo which, according to large-scale cosmological simulations, plays an essential part in their formation (Springel et al., 2005). Spiral galaxies may be grouped into various classes, the distinctions resting on how tightly wound the spirals are (Binney and Merrifield, 1998), and are sometimes labelled as ‘grand design’ or ‘flocculent’ depending on the coherence of the spiral arms. Figure 1.7 shows an example of a flocculent spiral galaxy. Lenticular galaxies, on the other hand, are regarded as intermediate between elliptical and spiral galaxies. They do not exhibit spiral arms but can form bars and rings.

### 1.3 SCALES, PARAMETERS, PHYSICAL MODELS

Disks encompass a vast range of scales and compositions but they all share the same fundamental force balance: the centrifugal force matches the radial component of the central

object’s gravity. The mutual cancellation of these powerful forces releases into the dynamical arena a host of subdominant processes that provide the inherent variety and interest of astrophysical disks (Gor’kavyj and Fridman, 1994). Some of these we cover later in this chapter. For now we provide a list of key scales and dimensionless quantities that help distinguish different disks from each other and determine which physical models are appropriate.

The physical quantities of most interest describe the geometry of the disk and its microphysics. We have met  $H$ , the vertical thickness or scaleheight of the disk, and  $r$ , the radius of the disk, earlier. In addition, the rotational angular speed of the disk is denoted by  $\Omega$ , the particles’ collision frequency by  $\omega_c$ , their velocity dispersion by  $c$ , and their size by  $a$ . Vertical hydrostatic balance implies that  $c \sim H\Omega$ . In a frame moving with the bulk velocity of the fluid, the particles’ mean free path is hence  $\lambda \sim (\Omega/\omega_c)H$ . All of these parameters vary within the disk, in particular with radial location.

Sufficiently dense and cool gaseous disks feature collision frequencies much greater than the rotation frequency,  $\omega_c \gg \Omega$ . It follows that the mean free path is significantly less than the disk scale height. In other words, the (vertical) Knudsen number is small:  $\text{Kn} = \lambda/H \ll 1$ . As a result, equilibrium microphysics is dominated by interparticle collisions; the phase space distribution of particles approaches a Maxwellian and the equations of fluid dynamics (or magnetohydrodynamics) are appropriate (Shu, 1992).

These relations are reversed in galactic disks, debris disks, and the tenuous plasma in the very hot regions around some black holes (Binney and Tremaine, 2008; Rees et al., 1982; Narayan et al., 1998). In these settings,  $\omega_c \ll \Omega$ , and so we have  $\text{Kn} \gg 1$ . Collisions between particles are infrequent and the familiar continuum descriptions break down. In particular, the thermal relaxation timescale is of order, or longer than, the dynamical timescale, leading to severe velocity anisotropies and unusual momentum and heat transport (e.g. Toomre, 1964; Braginskii, 1965; Lynden-Bell, 1967). Especially extreme environments are the surpassingly hot midplanes of AGN and X-ray binaries, where the ions and electrons collisionally decouple and possess temperatures differing by 3 orders of magnitude (Rees et al., 1982). The collective behaviour in these systems is determined by long-range gravitational interactions, in the cases of galactic and debris disks, and by electromagnetic fields, in the case of a collisionless plasma, and researchers must resort to an appropriate kinetic theory or  $N$ -body simulations.

Often planetary rings fall uncomfortably between these frameworks. Ring particles undergo some tens of collisions per orbit, and thus  $\omega_c \sim \Omega$  and  $\text{Kn} \sim 1$  (Araki and Tremaine, 1986; Wisdom and Tremaine, 1988). Of course, one can persist with hydrodynamic models for certain problems, but they cannot capture strong velocity anisotropies nor the non-Newtonian behaviour of the stress (Goldreich and Tremaine, 1978b; Latter and Ogilvie, 2006a). One must instead call upon an appropriate dense-gas kinetic theory or  $N$ -body simulations (see Chapters by Stewart and Salo), neither of which is straightforward to implement nor interpret.

Disk system	$r$	$H/r$	$T$ or $c$	$\omega_c/\Omega$	$n$
Protoplanetary disks	$> 100$ AU	0.05	10 – 3000 K	$10^7 - 10^{12}$	$10^9 - 10^{18}$ cm $^{-3}$
Dwarf novae	0.005 AU	0.01	$10^3 - 10^5$ K	$10^{10} - 10^{12}$	$10^{17} - 10^{20}$ cm $^{-3}$
AGN	$> 100$ AU	0.001	$10^5 - 10^{12}$ K	$10^{-6} - 10^{10}$	$10^{10} - 10^{17}$ cm $^{-3}$
Debris disks: dust	10 – 1000 AU	0.01-0.1	$10^4 - 10^5$ cm/s	$10^{-5} - 10^{-2}$	$10^{-12} - 10^{-9}$ cm $^{-3}$
Galactic disks: stars	10 – 100 kpc	0.01 – 0.1	$10^6$ cm/s	$10^{-8}$	0.1 – 100 pc $^{-3}$
Galactic disks: gas	10 – 100 kpc	0.001 – 0.01	$10 - 10^4$ K	$10^8$	$10^{-1} - 10^6$ cm $^{-3}$
Saturn’s dense rings	0.001 AU	$10^{-7}$	0.1 cm/s	10	$10^{-6}$ cm $^{-3}$

Table 1.1. *Characteristic scales and parameters of selected disk categories. Estimates are lifted from references given in Section 1.2. Here  $T$ ,  $c$ ,  $\omega_c$ , and  $n$  refer to temperature, velocity dispersion (or sound speed), collision frequency, and number density respectively. Ranges of protoplanetary disk properties are for radii between 0.1 AU and 100 AU. The AGN estimates include the main disk but not the broad-line region at radii  $\gtrsim 1000$  AU. The extremely hot temperatures (and consequent low collision frequencies) correspond to the radiatively inefficient inner disk around a  $10^7$  solar mass black hole. The galactic estimates are for the Milky Way, and do not include the extremely hot diffuse phase of the ISM.*

Dense rings possess an additional peculiarity: not only is the mean free path of order the vertical size of the system, so is the particle radius,  $a$ . Thus we have

$$\lambda \sim a \sim H,$$

or, formulated another way,  $R = a/H \sim 1$ , where  $R$  is the Savage–Jeffrey parameter of granular flow theory (Savage and Jeffrey, 1981). In short, the particles that constitute the disk are macroscopic bodies, another impediment to a continuum description. There is no astrophysical analogue for this situation, as even the largest bodies in debris disks, and certainly stars in galaxies, possess  $R \ll 1$  (Wyatt, 2008; Binney and Merrifield, 1998).

There are important dynamical consequences when  $\lambda \sim a \sim H$ . Excluded-volume effects impose not only an unusual equation of state, but also precipitate the vertical ‘splashing’ of particles out of the ring plane. In addition, the ring’s rheology undergoes a dramatic alteration: the *collisional* transport of momentum (from one particle to another during a collision) dominates over the standard *free streaming* or *translational* transport (by individual particles between collisions). The dependence of the latter on the system parameters and state variables is markedly different and leads to alternative instabilities and dynamics (Araki and Tremaine, 1986; Wisdom and Tremaine, 1988).

Next we consider the range of scales upon which dynamical phenomena can manifest. Gaseous disks almost always exhibit

$$r \gg H \gg l,$$

where  $l$  is the viscous scale, defined for most dynamical purposes by  $l = \sqrt{\nu/\Omega}$ , with  $\nu$  the kinematic molecular viscosity. Using  $\nu \sim \lambda c$ , we obtain the scalings

$$l \sim \sqrt{\lambda H} \sim (\Omega/\omega_c)^{1/2} H.$$

Another way to put this is in terms of the Reynolds number, defined by  $\text{Re} = H^2\Omega/\nu \sim H/\lambda \gg 1$ . In most gaseous disks, the gulf separating the disk radius  $r$  from the disk thickness  $H$  is much smaller than that between  $H$  and the viscous dissipation length  $l$ . For instance, in a protoplanetary disk at 1 AU,  $H/r \sim 0.05$ , and  $l/H \sim 10^{-5}$ . The Reynolds number is hence huge  $\sim 10^{10}$  (Armitage, 2011).

Contrast this with Saturn’s dense rings where

$$r \gg H \sim l,$$

and energy is dissipated on lengthscales of order the disk thickness  $H \sim a$ . There simply are no shorter meaningful scales. Planetary rings are low Reynolds number flows,  $\text{Re} \sim 1$ , even if their viscosity is more than four orders of magnitude less than that of a protoplanetary disk:  $10^2$  cm $^2$ /s versus  $10^6$  cm $^2$ /s (Tiscareno et al., 2007; Armitage, 2011).

How does this influence the dynamics? Consider the onset of instabilities. In many cases, the input of energy is on a lengthscale around  $H$ , and in gaseous disks, on scales consequently much larger than  $l$ . Because of this separation, instabilities typically saturate by initiating a *turbulent cascade* of energy to the distant dissipation scales, as this is the most efficient way to rid the system of the excess energy. Planetary rings make a striking contrast, because  $l$  is not far from the input scale  $H$ . Though the ring viscosity is comparatively tiny, the system is ‘controlled’ by dissipation, and instabilities saturate instead by *generating structure* — and there is a huge range of scales between  $H$  and  $r$  available in which to do so. The result may be chaotic and disordered, but it is categorically different from turbulence. Note that if there is a sufficient separation between  $H$  and  $r$ , gaseous disks can in principle exhibit structure on intermediate scales as well: for instance, modulations riding on small-scale turbulence (Johansen et al., 2009).

Finally, an important distinguishing property of gaseous disks, at least, is their ionisation fraction. Cold and poorly ionised disks undergo very different dynamics compared with partially and fully ionised disks (Blandford and Payne, 1982; Balbus and Hawley, 1991; Blaes and Balbus, 1994; Wardle, 1999). This issue is less relevant in comparisons with dense planetary rings, which are composed of mostly uncharged macroscopic particles, and are thus closer to decidedly hydrodynamic systems, such as the cold neutral regions (‘dead zones’) of PP disks (Gammie, 1996). However, the low-collisional dust in faint rings when charged does suffer dramatic qualitative changes wrought by electromagnetic effects. The spoke phenomenon in the B-ring is perhaps the most famous example, but periodic structures are also forced by Saturn’s magnetic field, and large-scale electromagnetic

instabilities have been postulated (Goertz and Morfill, 1988; Horányi et al., 2004, 2009, Hedman chapter).

## 1.4 FORMATION

Most disk formation routes draw on either (a) the collapse of a cloud of material, (b) the tidal disruption of a body, due to its close approach to another massive body, or (c) a physical collision. Similarly, ring formation scenarios fall into one of these three camps, and historically have strongly influenced, and been influenced by, the question of disk formation generally. In this section we briefly review the three ideas. See the Charnoz chapter for a more in-depth discussion.

The first scenario is particularly relevant for protoplanetary disks (Section 1.2.1), which form from collapsing dense cores within gravitationally unstable molecular clouds (McKee and Ostriker, 2007). Because the collapsing material usually carries non-zero angular momentum, it flattens out and ultimately forms a disk orbiting the protostar. Turbulence in the gas then processes the angular momentum and permits the remaining mass to fall upon the young star. Note that magnetic fields and non-ideal MHD probably control the early collapse phase, and possibly the ensuing turbulent state (e.g., Joos et al., 2012). A similar scheme was originally postulated for disk galaxies (Eggen et al., 1962), though now it is generally accepted that they form via a sequence of mergers followed by gas contraction into a disk (Searle and Zinn, 1978).

The early stages of Saturn’s formation involved a collapsing spinning blob of gas in the protosolar nebula, some of which must have found its way into a circumplanetary disk. One theory posits that Saturn’s rings are the icy leftovers of this disk, the gas long accreted or blown away (Pollack et al., 1976). In this scenario the rings are primordial, almost as old as the Solar System, and share a similar dynamical origin (on a much smaller scale) to their host protoplanetary disk. As explained in the Charnoz chapter, however, the theory has problems explaining their icy composition, in addition to the relative absence of darker material borne by impacting meteoroids (an indication of relative youth) (e.g. Estrada and Cuzzi, 1996). Perhaps most problematic is the question of angular momentum, which is being drained from the system by ballistic transport (amongst other processes), and which would ensure a lifetime shorter than that of the Solar System (Durisen, 1984).

The second class of disk formation scenarios appeals to the full or partial tidal disruption of a secondary object. As described by Roche in the 19th century, a body that orbits too close to a central mass will be pulled apart by the combined action of gravitational and centrifugal forces (Chandrasekhar, 1969). Examples of astrophysical disks that form from the disrupted material include those around supermassive black holes after a stellar disruption, and the debris surrounding polluted white dwarfs (described in Section 1.2.5). Related, less dramatic, examples are those associated with close binaries, where the secondary star overflows its Roche

lobe, and the resulting stream feeds an accretion disk around the primary (Section 1.2.2).

Roche’s theory, in fact, was originally applied to the formation of Saturn’s rings; he proposed that a moon had veered too close to Saturn and had been tidally disrupted. Recent work augmenting this theory includes that of Harris (1984) and Canup (2010). The latter, in particular, posits the tidal disruption of the icy shell of a differentiated Titan-sized body and the subsequent accretion of its rocky core; the theory then naturally accommodates the striking homogeneity of the rings. An explanation similar in some details has been proposed by Leinhardt et al. (2012) for the dense Uranian ringlets. The inward migration of the moons may be driven by interactions with the circumplanetary disk or tidal interactions with the planet. A recent passing comet may also have been disrupted in a similar fashion (Dones, 1991), but estimates of the cometary flux at Saturn suggest that this would be an exceptionally rare occurrence in the last billion years (Lissauer et al., 1988).

The third formation scenario involves collisions. The astrophysical objects most closely associated with this scenario are dusty disks around stars (Section 1.2.3). Because of collisional destruction and radiation pressure, this dust must be constantly replenished by continual but infrequent collisions between the larger bodies in the belt. Collision-based formation theories for Saturn’s dense rings have appealed to a *single* cataclysmic impact between two moons or between a moon and a comet, the latter event occurring during the late heavy bombardment (Pollack, 1975; Charnoz et al., 2009). Both scenarios inherit the problems of the homogeneous composition and apparent youthfulness of the rings. It is plausible, however, that the F-ring is the result of a recent impact between Prometheus and Pandora (Hyodo and Ohtsuki, 2015), and a similar event may be responsible for the Neptunian arcs (Smith et al., 1989).

A more direct analogy with debris disks is provided by the dusty rings in the Solar System. These include Saturn’s F-ring, whose dust is continually supplied by the collisions between embedded larger bodies (Cuzzi and Burns, 1988; Barbara and Esposito, 2002). They also include Saturn’s G-ring, Methone, Pallene, and Anthe rings, in addition to the Jovian dust rings. For the most part, the dust in the latter disks issues from collisions between extrinsic impactors (micrometeoroids) and embedded large bodies, such as atmosphere-free moons (Hedman et al., 2009, 2010; Burns et al., 1999).

Finally, we mention Saturn’s E-ring and Io’s plasma torus, both volcanic in origin, for which there are no perfect extrasolar analogues. Very recent observations, however, show short-lived arcs of material around close-in exoplanets, ejected from their atmospheres or surfaces (van Lieshout et al., 2014; Sanchis-Ojeda et al., 2015).

## 1.5 ACCRETION

Once an astrophysical disk has formed, its subsequent evolution and ultimate dissipation are, to a large extent, dominated by accretion. Disks have a finite lifetime and ulti-



mately fall onto their central object via a process of angular momentum redistribution. The exceptions are galactic and debris disks. In this section we focus on accretion driven by local angular momentum transport, such as turbulence or interparticle collisions. Note that other mechanisms exist that are important in certain circumstances, such as magnetocentrifugal winds, or large-scale waves (Pudritz et al., 2007; Balbus and Papaloizou, 1999).

### 1.5.1 Gaseous disks

The classical theory of accretion disks (e.g. Lynden-Bell and Pringle, 1974; Pringle, 1981) describes the evolution of a (more or less) continuous disk or ring of matter in circular orbital motion around a massive central body. Any dissipative process that acts similarly to a frictional or viscous force causes the inner parts of the disk, which rotate more rapidly, to transfer angular momentum to the outer parts. The disk spreads as its inner and outer parts move to smaller and larger orbital radii consistent with their specific angular momentum. Alongside this outward transport of angular momentum there is a net inward transport of mass. Meanwhile the orbital energy of the disk is lowered and heat is generated which, once radiated and intercepted by astronomical instruments, yields some of the observations described in Section 1.2. Ultimately the disk will fall upon the central object in a time of roughly  $\sim r^2/\nu$ , where  $r$  is the disk's outer radius. According to this estimate Saturn's rings will be gone in  $10^{10}$  years, longer than the age of the Solar System. In contrast, if the only momentum transport process in PP disks was molecular viscosity, they would survive for some  $10^{16}$  years, longer than the age of the Universe! To explain the observations in PP disks at least, an effective, or 'anomalous', viscosity must be present at a much greater magnitude, some  $10^{16} \text{ cm}^2/\text{s}$ .

Within the astrophysical disks mentioned in Section 1.2, several different mechanisms of angular-momentum transport may be operating. Some gaseous disks are sufficiently hot that the main constituents are substantially ionised; these include the disks around black holes and compact stars in interacting binary systems (at least during their actively accreting phases), and the protostellar disks of FU Orionis systems. In these systems the magnetorotational instability (MRI; Balbus and Hawley, 1991, 1998) is expected to sustain a dynamically significant magnetic field and to provide measurable angular-momentum transport through magnetohydrodynamic turbulence. In cooler disks, such as typical protoplanetary systems, where the degree of ionisation is much lower, the MRI may be restricted only to special regions of the disk (see for example Gammie, 1996; Armitage, 2011). Other, purely hydrodynamic mechanisms have been proposed to permit sustained activity in magnetically dead regions. These include turbulence instigated by gravitational instability ('gravitoturbulence'; see Section 1.8.1), which may attack the more massive early stages of PP disks (Papaloizou and Savonije, 1991; Durisen et al., 2007), subcritical baroclinic instability (Lesur and Papaloizou, 2010b), vertical shear instability (Nelson et al., 2013; Barker and Latter,

2015), and vertical convection (though it may be difficult to self-sustain; Lesur and Ogilvie, 2010).

In situations where a plausible mechanism of angular-momentum transport has been identified, the difficulty remains of quantifying its efficiency. Most transport processes are stochastic in nature, but what is needed for the global evolution of the disk is the mean value of the shear stress and its dependence on relevant quantities such as the density, pressure, shear rate, etc. Shakura and Sunyaev (1973) introduced a useful parametrisation in which the shear stress is written as the pressure multiplied by a dimensionless parameter  $\alpha$ . In the case of hydrodynamic or magnetohydrodynamic turbulence,  $\alpha$  is expected to lie between 0 and 1 if the perturbations of the fluid velocity (and Alfvén velocity, in the MHD case) are related to the sound speed (but typically less than it). This 'alpha-disk' prescription has dominated accretion-disk theory for some 40 years, as it permits researchers to construct models of disk evolution and structure, and hence generate synthetic emission spectra that can be compared with observations.

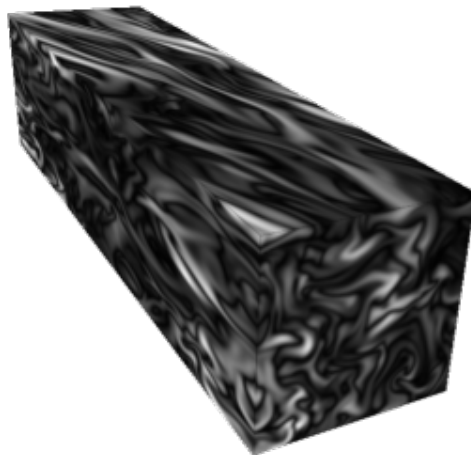


**Figure 1.8** A snapshot from a simulation of MRI turbulence conducted in the shearing box model of a gaseous accretion disk. The field plotted is the magnetic field strength  $|\mathbf{B}|$ . Credit: Tobias Heinemann.

The turbulent state can be investigated through numerical simulations of a relevant system of hydrodynamic or magnetohydrodynamic equations. If the disk is thin and the correlation length of the turbulence is small compared to the orbital radius, then a local simulation based on the shearing box (e.g. Hawley et al., 1995) is usually sufficient; the shear stresses can be measured directly from the simulation. Figure 1.8 presents a snapshot from a local simulation of the MRI. Attempts have also been made to describe the turbulent state analytically by means of a set of moment equations derived from the basic hydrodynamic or magnetohydrodynamic equations using a closure model, such as a simple modelling of the triple correlations of velocity and magnetic fluctuations (Kato and Yoshizawa, 1993, 1995; Ogilvie, 2003).

### 1.5.2 Rings

In the case of planetary rings, angular momentum is transported in part by a viscous stress associated with an anisotropic velocity distribution of the particles, and therefore with an anisotropic pressure tensor (free-streaming transport). Indeed, the  $\alpha$  viscosity parameter of a dilute planetary ring (and also a dilute plasma) can be linked to the degree of anisotropy in the pressure tensor. In dense rings, however, there is an additional contribution from the transport of angular momentum during (rather than between) collisions.

There is a close analogy between the behaviour of the pressure tensor in a dilute planetary ring and the Reynolds stress tensor that describes the correlations of velocity fluctuations in a turbulent gaseous disk (Quataert and Chiang, 2000). These tensors obey evolutionary equations with some identical terms, describing the interaction of the fluctuations with the Keplerian orbital motion (which tend to make the tensor anisotropic), as well as some differing terms, describing the collisional and nonlinear dynamics. In the case of a dilute planetary ring, collisions make the pressure tensor isotropic and damp the fluctuations. Goldreich and Tremaine (1978b) showed that a circular dilute equilibrium can be sustained if the collisions are sufficiently elastic. Similarly, in purely hydrodynamic turbulence, the nonlinear effects tend to both isotropise and damp the velocity fluctuations. Sustained hydrodynamic turbulence is possible only if the isotropisation is relatively strong compared to the damping, a condition that is not believed to be satisfied in a Keplerian disk (Ogilvie, 2003). Note that additional thermal gradients may permit sustained activity.

An additional complication is that planetary rings, like gaseous disks, can suffer instabilities that lead to disordered flows on large scales ( $> H$ ), e.g. gravitational instability (Salo, 1992, 1995). The correlated motions of the associated turbulence transport angular momentum up to an order of magnitude greater than both the free-streaming and collisional stresses (Daisaka et al., 2001). This transport can also be parametrised by an alpha prescription, though such a model must omit the complicated interplay between the turbulent wakes and the collisional dynamics of the ring particles, the length and timescales of which are not well separated. Plasma systems that undergo analogous mixed behaviour involving ‘micro-turbulence’ are the solar wind, the intracluster medium, and the inner regions of black-hole accretion disks (e.g. Kunz et al., 2014).

The alpha model, and more sophisticated approaches, are mean-field theories in which the details of the small-scale physics (turbulent motions, collisions) are deemed quasi-steady and averaged away. However, for certain astrophysical processes this microphysics cannot be treated so indifferently. Planet formation and dust production, in protoplanetary and debris disks respectively, rely on the details of collisional disruption and agglomeration, which are also relevant for both dense and dusty planetary rings. In the next section we review these processes.

## 1.6 COLLISIONS AND DUST

The collisional dynamics of Saturn’s and Uranus’s macroscopic ring particles are unusual in astrophysics on account of their low impact speeds  $\sim$  mm/s. In fact, these are of order the escape speeds from the larger particles, and only enhanced tidal forces (due to their orbit) prevent gravitational collapse. Solid bodies in debris or protoplanetary disks collide more violently on the whole, at speeds ranging between mm/s and km/s. Nevertheless, there is significant overlapping physics that is instructive to review. We also discuss in this section the connections between the dynamics of dust in debris disks and the tenuous rings of the Solar System.

### 1.6.1 Planet formation

The theory of planet formation tracks the agglomeration of solid particles in disks from micron-sized dust to the  $10^3$  km cores of giant planets. Vaulting this tremendous gulf, spanning some 12 orders of magnitude, requires multiple growth mechanisms and physical processes.

Microgravity experiments show that impacts between sub-centimetre dust grains are controlled by their coupling with the ambient gas and generally result in sticking collisions, whether their motions are Brownian or induced by turbulence (Blum and Wurm, 2008). Typical impact speeds are of order 1 m/s (Brauer et al., 2008) and attractive surface forces are relatively strong in this regime. Larger particles are only weakly coupled to the surrounding gas flow and thus achieve greater impact speeds, meaning surface forces become less dominant. As a consequence, collisions are more likely to result in bouncing or fragmentation, not sticking, and agglomeration to sizes larger than centimetres is difficult. Note that these details are complicated by particles’ structure (how ‘fluffy’, how compacted, etc.) and their composition (silicate versus icy, for instance) (Testi et al., 2014). Especially interesting are collisional outcomes between solids of disparate sizes, which sometimes result in a net mass transfer to the larger particle. Hence there may exist a narrow route by which a small number of ‘lucky’ aggregates can grow to km sizes, leaving behind a swarm of small ‘unlucky’ grains (Wurm et al., 2005; Testi et al., 2014).

In conjunction with laboratory experiments, numerical simulations, using  $N$ -body molecular dynamics and SPH, have determined collisional outcomes between aggregates of up to decimetre sizes (Wada et al., 2008; Geretshauser et al., 2010; Ringl et al., 2012; Seizinger and Kley, 2013). Figure 1.9 shows the outcome of such a simulation. Additionally, statistical information has been gleaned from integration of suitable coagulation equations (e.g. Safronov, 1969; Dohnanyi, 1969; Tanaka et al., 1996) that evolve forward in time the distribution function of a swarm of colliding dust grains (e.g. Dullemond and Dominik, 2005; Windmark et al., 2012; Garaud et al., 2013). In such calculations, collisions are parametrised in a mathematically convenient but also physically motivated way.

The growth of larger bodies, from centimetre to kilometre sizes, is an especially active area of research. Most theories rely at some point on the gravitational collapse of many

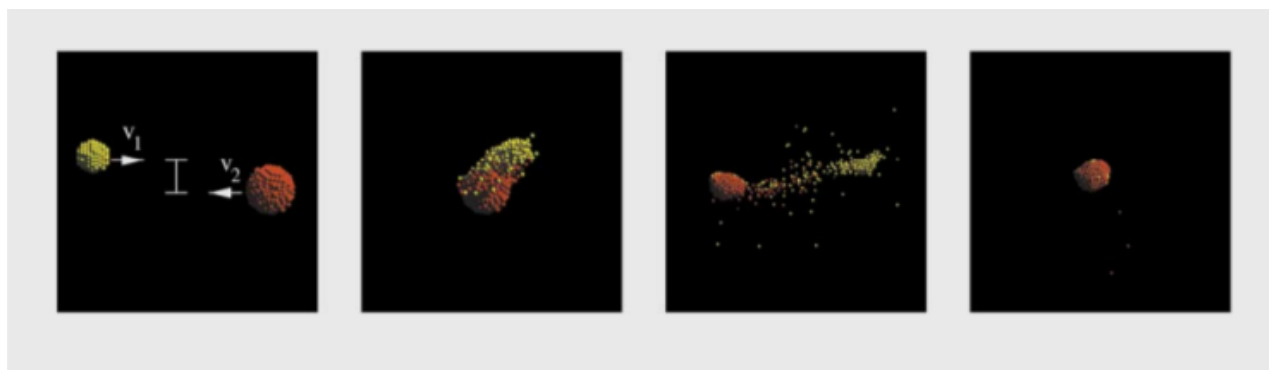


**Figure 1.10** Snapshots before, during, and after a collision between two planetesimals using an  $N$ -body simulation. Credit: Leinhardt and Richardson (2002).

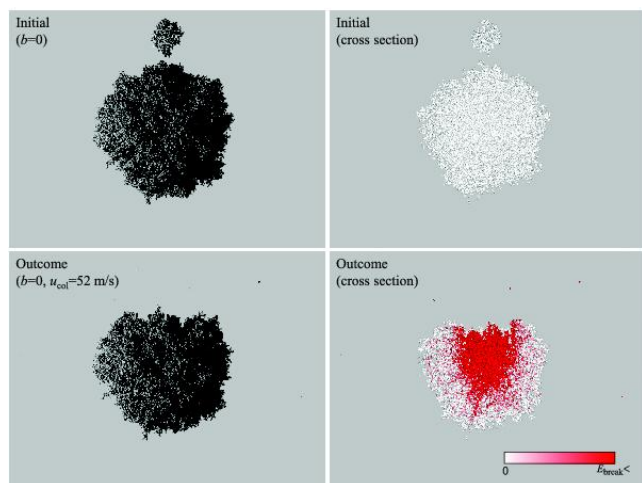


**Figure 1.9** Snapshots before and after a simulated collision between dust aggregates. The red shading in the right panel indicates the amount of energy dissipated during the impact. The number of spherical components in each cluster is 2000 and 128,000 respectively. The impact speed is 52 m/s. Credit: Wada et al. (2013).

particles, usually in collaboration with aerodynamical effects: streaming instability; accumulation in ‘dust traps’, such as zonal flows and disk vortices; ‘pebble accretion’, etc. (Youdin and Goodman, 2005; Barge and Sommeria, 1995; Lambrechts and Johansen, 2012). The robustness and efficiency of these various mechanisms are still unclear.

Solid bodies above roughly a kilometre (called planetesimals) are decoupled from the gas and further coagulation is achieved by direct collisions, the frequency of which is aided significantly by gravitational focusing (Papaloizou and Terquem, 2006). Numerical SPH and  $N$ -body simulations have probed the outcomes of their collisions and show that they fall into a variety of regimes: cratering, merging, fragmentation, ‘hit-and-run’, and annihilation (Leinhardt and Stewart, 2012). These regimes partly depend on whether the bodies are held together by tensile strength or self-gravity. Figure 1.10 shows snapshots of a simulation of a high-velocity collision between two planetesimals.

The collective dynamics of a swarm of planetesimals may be modelled with a suitable coagulation equation or  $N$ -body simulation (see e.g. Wetherill and Stewart, 1993; Kokubo and Ida, 1996; Weidenschilling et al., 1997; Richardson et al., 2000). These typically indicate runaway growth of a few aggregates which halts upon reaching 1000 km sizes (Greenberg et al., 1978; Wetherill and Stewart, 1989). The resulting planetary ‘embryos’ or ‘protoplanets’ continue to accrete, albeit at a much reduced rate, via what is termed oligarchic growth (Kokubo and Ida, 1998).

### 1.6.2 Debris disks

If researchers in planet formation focus almost exclusively on how large objects are assembled from dust grains, one could say researchers of debris disks take the diametrically opposed viewpoint: how do large bodies produce the observed tiny grains? In fact, the process of runaway accretion in planetesimal belts produces not only larger objects, but also significant quantities of dust (Kenyon and Bromley, 2004a,b). Dust production hence continues well after the disk gas dissipates and throughout the intermittent collisional evolution of the ‘leftover’ planetesimals and protoplanets (Wyatt, 2008; Matthews et al., 2014).

In contrast to the coagulation equations employed in planet formation, researchers compute the statistical distribution of debris disk solids with collisional cascade models. The largest bodies ( $\sim 1 - 100$  km) are input as ‘fuel’, and mass is lost at the smallest sizes due to radiation effects and collisional destruction. The resulting wide dynamical range, some 40 orders of magnitude in mass, makes these calculations especially difficult. The simplest models assume a steady-state size distribution but with decreasing total mass (Dominik and Decin, 2003). For detailed comparison with observations, however, more advanced variants are needed that include, for instance, the particles’ orbital elements, and use kinetic theory (Krivov et al., 2006; Löhne et al., 2012) or ‘particle in a box’ methods (e.g. Thébault and Augereau, 2007).

$N$ -body codes that track explicitly each member of a small subset of the solids have been useful in simulating the effects of large perturbations on disk structure, such as those arising from an embedded planet. They struggle, however, to

explain the overall distributions. Hybrid codes have emerged recently that comprise  $N$ -body simulations coupled to dust evolution, thus describing both dynamics and collisions accurately and concurrently (Kral et al., 2013; Nesvold et al., 2013). The codes evolve forward in time the properties of a cloud of similarly sized particles on the same orbit ('superparticles'). Collisions between these groups generate new superparticles that represent the post-collisional fragments (Matthews et al., 2014).

### 1.6.3 Rings

As in the fields of planet formation and debris disks, the collisional dynamics of planetary ring particles has been explored with laboratory experiments and statistical methods. The overwhelming majority of work, however, has been undertaken with  $N$ -body simulations. Owing to numerical limitations, these have focused on shorter time-scale dynamical phenomena such as the onset of instabilities and satellite wakes (Salo, 1991; Salo et al., 2001; Lewis and Stewart, 2000, 2009), rather than on the slower processes that shape the particles' size distribution. Most  $N$ -body studies of dense rings involve hard indestructible spheres, either identical or with a fixed distribution of sizes. Collisions are controlled by a normal coefficient of restitution, and a tangential coefficient of restitution when including the particle spin. See Chapters by Stewart and Salo for further details. Needless to say, the regime of frequent and gentle collisions, which characterises dense rings, is very remote from the contexts described previously in this section.

Because of the low impact speeds, proximity to the planet, and the properties of the particles' regolith, a myriad of processes control the evolution of the size distribution in dense rings. In addition to inelastic 'bouncing' (modelled in  $N$ -body simulations), collisions may lead to: adhesion (due to the meshing of micron-sized surface structures or more drastic structural reconfigurations); surface compaction of loose frost ('polishing'); mass transfer between impacting particles; as well as the more familiar collisional fracture. Laboratory experiments have been essential in uncovering and characterising these various effects (e.g. Bridges et al., 1984; Hatzes et al., 1988, 1991; Supulver et al., 1995, 1997, Colwell Chapter). A raft of non-collisional processes also contribute. These include gravitational recapture of collisionally dislodged fragments, tidal fragmentation, rotational fragmentation, and erosion by micrometeoroid impacts (Weidenschilling et al., 1984). This miscellany of physics includes effects present in protoplanetary dust dynamics (bouncing, adhesion, polishing, fragmentation) and planetesimal dynamics (rotational fracture, gravitational recapture), as well as new effects (tidal fracture, micrometeoroid bombardment).

In parallel to laboratory experiments, theoretical descriptions of individual collisions have been developed that employ viscoelastic theories (e.g. Spahn et al., 1995; Albers and Spahn, 2006a). On the other hand, computing the energetics of variously packed aggregates can characterise collisional outcomes as a function of impact speed (Guimarães et al., 2012). Future work, involving  $N$ -body or molecular dynam-

ics simulations (as with planetesimals; Leinhardt and Stewart, 2012), may categorise collisional events more securely.

There exist a small number of statistical studies exploring the cumulative effect of collisional coagulation and fragmentation, such as Weidenschilling et al. (1984), Longaretti (1989), and more recently Bodrova et al. (2012) and Brilliantov et al. (2015). Finally, 'sticky' collisions have been modelled in a restricted set of  $N$ -body simulations that numerically produce self-consistent size distributions in relatively good agreement with observations (Perrine et al., 2011; Perrine and Richardson, 2012). In comparison with the field of planet formation, however, this area of research, though very promising, is underdeveloped. For example, no well-defined 'barriers' have been computed above which growth of large aggregates halts, and below which small particles are efficiently swept up by larger ones. Nor have calculations been attempted that could decide if it is statistically likely that a few 'lucky' aggregates could grow to very large sizes  $\sim 100$  m (as in planet formation theories). If such growth was possible, it may provide an explanation for the observed propellers in Saturn's A-ring (see Spahn chapter).

The collisional dynamics of Saturn's F-ring differs from that of the inner dense rings. The F-ring consists of a belt of large  $\sim 1$  km bodies swathed in the dust generated by their mutual collisions (Cuzzi and Burns, 1988; Colwell et al., 2009; Attree et al., 2012; Meinke et al., 2012). The larger bodies are possibly the fragments of a catastrophic collision between Prometheus and Pandora (Hyodo and Ohtsuki, 2015) that are in the slow process of being ground down collisionally (Cuzzi and Burns, 1988), a scenario directly analogous to models of debris disks. Neptune's dusty rings, which are far less well studied, probably share a similar formation history and similar dynamics (Smith et al., 1989). Another connection is the powerful influence of a nearby satellite. Prometheus significantly 'stirs' the F-ring material, enhancing the collision rates of the  $\sim$  km sized moonlets and perturbing the overall structure of the ring in much the same way that embedded or nearby planets shape the dust in debris disks (Murray et al., 2005; Beurle et al., 2010; Attree et al., 2014).

One of the essential features of the F-ring is its weaker tidal environment, as compared to the inner dense rings. Gravitational aggregates at smaller radii have difficulty growing to large sizes before they are tidally disrupted (an interesting contrast to debris disks and planetesimal belts). This has stimulated alternative theories for F-ring dynamics that posit that the population distribution is quasi-static, the number of large bodies regulated by fragmentation and gravitational accretion (Barbara and Esposito, 2002). Indeed it is true that  $N$ -body simulations show F-ring particles readily clump into gravitationally bound aggregates, akin to 'rubble piles' (Karjalainen and Salo, 2004; Latter et al., 2012b), whose further growth and collisional destruction characterise the general dynamics (Karjalainen, 2007; Hyodo and Ohtsuki, 2014). The collective outcome of aggregation and disruption has been theoretically explored using statistical methods similar to those employed in other astrophysical disks (Barbara and Esposito, 2002; Esposito et al., 2012). There remains, however, plenty of scope to further ap-

ply the well developed techniques of debris disks and planet formation to this problem.

### 1.6.4 Radiation and other forces

In debris disks, radiation forces (Burns et al., 1979) play an important role in the dynamics of small particles. Often a distinction is made between radiation pressure and Poynting–Robertson (PR) drag, although the origin of the two effects is the same (photons transferring energy and momentum to dust grains). Radiation pressure removes micron-sized dust grains from the system on a dynamical timescale, thus enforcing a strict lower cut-off in the size distribution of solids (Wyatt, 2008). PR drag, on the other hand, causes small particles to spiral into the central star, but on a timescale longer than collisional erosion. It is hence far less important (Wyatt, 2005b).

In contrast, the PR drag on planetary ring particles can lead to rapid inward migration of dust (Goldreich and Tremaine, 1982), especially an issue in the F-ring and Saturn’s diffuse rings (Sfair et al., 2009; Verbiscer et al., 2009). This is less important in the inner dense rings where the dust is partially shielded from the Sun and its dynamics controlled by collisions with larger particles. The scarcity of sub-mm dust in dense rings can be attributed to their efficient absorption by larger particles (Becker et al. 2016, French and Nicholson, 2000).

Ring dust is also subject to drag forces issuing from both the host planet’s exosphere and the dilute plasma coorbiting with its magnetosphere. As a result, dust can feel either a headwind or tailwind that causes radial migration and eventual loss from the system, an effect remarkably similar to the aerodynamical migration experienced by centimetre to metre-sized particles in protoplanetary disks (Weidenschilling, 1977). Uranus’s outer atmosphere is especially extended (Broadfoot et al., 1986), explaining the paucity of dust in its ring system, and which may also have some dynamical consequences on ringlet confinement (Goldreich and Porco, 1987a). Charged dust elevated above Saturn’s main rings, on the other hand, interacts with the Saturnian magnetosphere leading to radial drifts, angular momentum exchange, potential instability, and the striking spoke phenomenon (Goertz and Morfill, 1988; Horányi et al., 2004, 2009).

## 1.7 WAVES

The study of waves (and instabilities) in astrophysical disks began with attempts to explain the appearance of spiral structure in galactic disks (Toomre, 1964; Lin and Shu, 1964; Goldreich and Lynden-Bell, 1965). The observed spirals may be interpreted as ‘density waves’, a collective phenomenon combining inertial (epicyclic) forces and self-gravity, but strongly influenced by the orbital shear. Density waves have also been studied in gaseous disks, where they can be thought of as inertial–acoustic waves because pressure usually dominates self-gravity, leading to qualitative

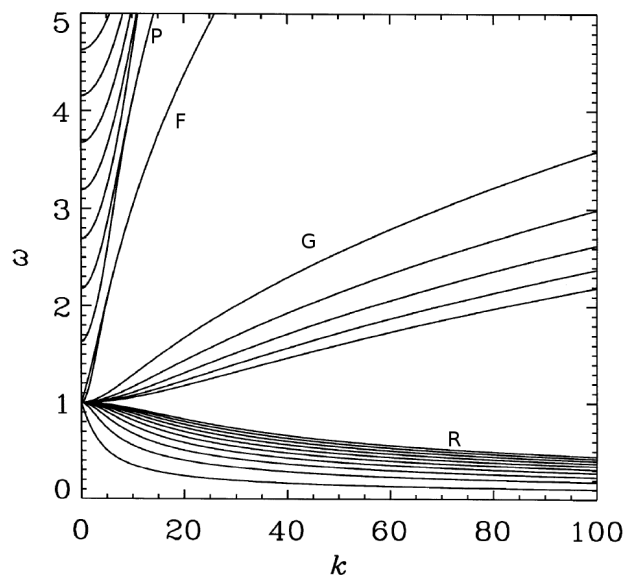


**Figure 1.11** The dispersion relations of the first few axisymmetric p, f, g, and r modes in a local model of a disk. The frequency of the modes  $\omega$ , scaled by  $\Omega$ , is plotted versus radial wavenumber  $k$ . The disk is a stably stratified polytrope. Credit: Ogilvie (1998).

differences in their propagation (the group velocity differs in sign, for instance).

If the viscosity parameter  $\alpha \ll 1$ , then gaseous disks manifest a variety of additional wave modes with wavelengths comparable to or less than  $H$ . Such waves are only accurately studied in three-dimensional models that resolve the disk’s vertical structure (Loska, 1986; Okazaki et al., 1987; Lubow and Pringle, 1993; Korycansky and Pringle, 1995; Ogilvie, 1998). The disk may then be understood as a wave guide through which the various modes propagate. In some models the hydrodynamic waves can be classified into f (fundamental), p (pressure) and g (gravity) modes by analogy with stellar oscillations (Ogilvie, 1998). Rotation also introduces low frequency r modes (also called ‘inertial waves’). Example dispersion relations of these modes are plotted in Figure 1.11. Global oscillations can be formed when these waves reflect from radial boundaries of the disk or internal turning points. The study of this rich assortment of modes is sometimes called ‘diskoseismology’. One of its aims has been to explain the curious quasiperiodic oscillations (QPOs) exhibited by certain X-ray sources (Remillard and McClintock, 2006), then use these to probe the relativistic gravitational fields associated with black holes and neutron stars (e.g. Wagoner, 1999).

The symmetric f modes exhibit the least vertical structure and correspond to the spiral density waves observed in galaxies and PP disks, in addition to the large-scale eccentric modes inferred in both close binaries and certain PP disks. In addition, antisymmetric f modes can manifest as bending waves, which transmit a warp (or vertical deformation) through the disk (Papaloizou and Lin, 1995; Ogilvie, 1999, 2006). Vertical tilts and warps, in fact, have been observed in X-ray binaries, AGN, and protoplanetary disks,



and are usually driven by a misaligned companion (Katz, 1973; Kotze and Charles, 2012; Miyoshi et al., 1995; Marino et al., 2015b).

In planetary rings the smallest meaningful lengthscale is the particle size  $\sim H$  and hence wave modes express little to no vertical structure: the disk is effectively two-dimensional. As a consequence, planetary rings cannot support nearly the same variety of waves as gaseous disks, and in fact only the  $f$  modes are present. The *Voyager* and *Cassini* spacecraft imaged many examples of spiral density and bending waves excited in Saturn’s A-ring and B-ring by the planet’s moons (Colwell et al., 2007). Their physics is very similar to the case of close binaries and embedded planets in PP disks (see Section 1.9).

In contrast, some density waves located in the C-ring may have been generated by low-order normal-mode oscillations within Saturn itself (Marley, 1991; Hedman and Nicholson, 2013; Fuller, 2014). The study of such waves (‘kronoseismology’) may provide clues about the internal structure of the central planet. This effort provides a nice parallel to diskoseismology’s attempts to characterise black holes and neutron stars.

Large-scale ‘corrugation waves’ with wavelengths  $> 30$  km have also been observed in the C and D-rings generated by a cometary impact dating from the 1980s (Hedman et al., 2007, 2011). Similar waves were excited in Jupiter’s main ring by Shoemaker–Levy 9 in 1994 (Showalter et al., 2011). In fact, an analogue of this process occurs in young protostellar disks: infalling material from the star’s natal envelope can cause spiral shocks in the disk, which may transport a non-trivial amount of angular momentum, while thermally processing chondrule precursors (Boss and Graham, 1993; Lesur et al., 2015). An important distinction, however, is that the collective forces are far more significant in gaseous disks, so that the disturbances are bonafide waves, unlike in the ring context, where the structures are essentially kinematic.

The observed spiral waves in planetary rings possess radial wavelengths that are much greater than the thickness of the rings  $> 10$  km, and this means that self-gravity dominates pressure (or velocity dispersion) in their propagation, while the viscosity of the rings usually damps the waves. But density waves have been observed on much shorter scales as well. Both axisymmetric and non-axisymmetric density structures appear with roughly 100 m wavelengths in RSS, UVIS, and VIMS observations (Thomson et al., 2007; Colwell et al., 2007; Hedman et al., 2014). The small-scale non-axisymmetric wakes, in particular, give rise to a striking large-scale effect, the azimuthal brightness asymmetry (Camichel, 1958; Colombo et al., 1976; Thompson et al., 1981; Salo, 1992).

In order to reach dynamically important (and observable) amplitudes, waves must grow to nonlinear strengths. As mentioned, periodic forcing due to an orbiting companion naturally excites waves and other, non-propagating, disturbances. This is reviewed in Section 1.9. Conversely, numerous instabilities can drive wave (and other) activity to observable levels. Relevant instabilities are discussed in the following section.

## 1.8 INSTABILITIES

Because of their physical complexity, gaseous accretion disks accommodate a large number of instabilities, usually drawing their energy from the background orbital shear but sometimes also from vertical shear, thermodynamic gradients, or directly from the self-gravitational potential of the disk. It might be said there are more instabilities than observations they could feasibly explain! This is in contrast to Saturn’s dense rings where there is an abundance of observed structure, much of it presumably generated by instabilities not yet identified or understood. In the following subsection we review only those processes that are shared by, or have something in common with, those appearing in planetary rings.

### 1.8.1 Gravitational instability and gravitoturbulence

As explained in the Stewart chapter, self-gravity decreases the squared frequency of density waves, leading to axisymmetric instability on intermediate wavelengths when Toomre’s parameter  $Q = \kappa c / \pi G \Sigma < 1$  (Toomre, 1964). Here  $\kappa$  is the disk’s epicyclic frequency and  $\Sigma$  is its surface density. Note that the criterion given here is for a two-dimensional gaseous disk, and differs slightly in other models. The above condition can plausibly be met in spiral galaxies, more massive PP disks, accretion disks in active galactic nuclei, and, of course, dense planetary rings.

Gravitational instability (GI) is thought to power the density waves observed in flocculent spiral galaxies (and possibly grand design spirals), and thus controls a crucial aspect of their structure. Observed spirals in protostellar disks may share the same origin, though embedded planets could also drive these features. GI also features in the ‘disk instability’ theory of planet formation, by which gas giants are formed by direct collapse of the disk (Kuiper, 1951; Cameron, 1978; Boss, 1998). In planetary rings, GI is responsible for ‘wake’ activity on much smaller relative scales, on account of the extreme thinness of the rings. Because unstable waves emerge on scales  $\gtrsim H$ , they are usually global features in gaseous disks and local features in planetary rings.

Unstructured disks are linearly stable for  $Q > 1$ , as they cannot support non-axisymmetric GI modes. However, for somewhat larger  $Q \approx 2$ , finite-amplitude perturbations instigate sustained spiral density waves and the system settles into a ‘gravitoturbulent’ state. Figure 1.12 shows a snapshot of GI-induced turbulence in a local model of a gaseous disk; here the mean  $Q$  is 2.5. At least locally, this is a ‘subcritical’ transition: the disk can support both a laminar and a turbulent state for  $1 < Q \lesssim 2$  but leaves the laminar equilibrium when given a sufficiently vigorous perturbation. In practice, the critical amplitude is small; the shot noise inherent in  $N$ -body simulations is always sufficient to disrupt the laminar state.

The nonlinear outcome of gravitational instability is sensitive to heating and cooling because  $Q$  is proportional to the velocity dispersion, or sound speed, of the disk. Typically the instability leads to enhanced dissipation that tends to increase  $Q$ , so a thermostatic regulation can be achieved

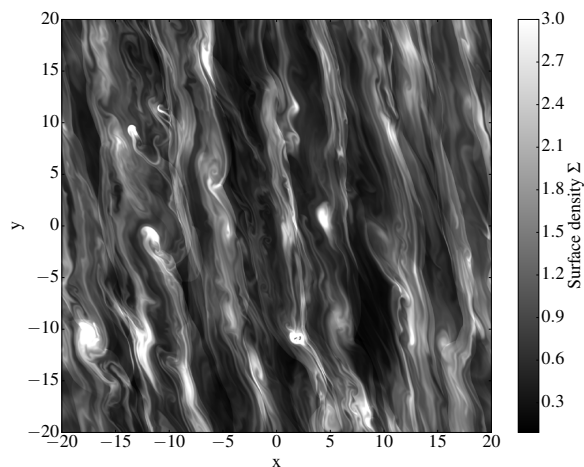


**Figure 1.12** Gravitoturbulence in a 2D shearing box model of a gaseous disk. The fractional surface density perturbation is plotted, while the unit of length is the initial unperturbed scale height  $c/\Omega$ , which here is five times the Jeans length  $G\Sigma_0/\Omega^2$ , where  $\Sigma_0$  is the mean surface density. The (linear) cooling time is  $9/\Omega$ . Credit: Antoine Riols-Fonclare.

in which  $Q \sim 1$  and a stochastic field of density waves maintained. Such an equilibrium has been obtained in local numerical simulations of gaseous disks (Gammie, 2001), and the resulting turbulence has properties in common with states found in simulations of self-gravitating planetary rings (e.g. Salo, 1995; Daisaka et al., 2001), even though the cooling processes differ. One important issue for accretion disks has been the question of turbulent angular-momentum transport by GI. Can gravitoturbulence provide an effective alpha, as required by the Shakura-Sunyaev theory? While it certainly can lead to accretion, it is not always assured that GI dissipates energy locally because of its wavelike character (Balbus and Papaloizou, 1999), though this seems to be only an issue for thicker disks (and certainly not for planetary rings).

If the disk is permitted to cool on a timescale that is sufficiently short compared to the orbital timescale, then the disk may fragment and form a number of bound objects (stars, planets, moonlets, etc). In recent years, much effort has gone into determining the critical cooling time from hydrodynamical simulations (e.g. Johnson and Gammie, 2003; Rice et al., 2005; Durisen et al., 2007). The question is still open, as it is increasingly clear that the problem is sensitive to the numerical details of the calculations (Paardekooper, 2012; Rice et al., 2014). Clumps also form in local simulations of planetary rings (e.g. Karjalainen and Salo, 2004), especially at larger radii where the tidal forces are weaker. Generally, however, stable clumps are more difficult to form in rings, in part because the minimum lengthscale  $a$  is  $\sim H$ , and clumps are thus easier to be ripped apart by tidal forces and/or collisions with other particles (or wakes) than the much smaller gaseous cores. Another way to think about this is in terms of the equation of state, or a change of phase. Gravitational collapse, in any system, should end once material becomes so dense that pressure resists infall and/or its cooling radically diminishes (via an opacity jump, for example). In gaseous

disks the lengthscale upon which collapse halts is exceptionally small  $\ll H$ , whereas in planetary rings it is  $\sim H$ . Once ring material clumps it almost immediately becomes ‘incompressible’: it changes state from a ‘granular gas’ to a ‘granular liquid’. In addition, cooling is minimised because within a crowded aggregate ‘collisions’ are very gentle (if not absent) and hence more elastic. Nonetheless, clump formation is an important feature in the outer A-ring and in the F-ring, where there is indeed a population of larger objects, ‘propellers’ and ‘kittens’ respectively (see Section 1.6.3 and chapters by Spahn and Murray).

### 1.8.2 Viscous overstability

A viscous stress need not just damp density waves (or  $f$  modes), it can also, somewhat counterintuitively, cause such waves to grow. A density wave produces stress perturbations that couple the background orbital shear to the wave velocities. Energy is extracted and the wave amplified if the velocity and stress oscillations are sufficiently in phase. The instability typically saturates in a quasi-steady state, with the viscous driving of the waves balanced by their viscous destruction (see Stewart chapter). The process was first discovered in the accretion-disk context (Kato, 1978; Blumenthal et al., 1984), where it was hoped it might explain observed luminosity fluctuations around compact objects.

As with density waves excited by GI, viscously overstable modes, and their saturation, are essentially global in the accretion disk context. Thus the inner and outer boundaries, Lindblad resonances, and the disk’s vertical structure all feature in the evolution of the instability (Papaloizou and Stanley, 1986; Kley et al., 1993; Miranda et al., 2015). In contrast, viscous overstability in planetary rings can be a very local phenomenon — certainly when axisymmetric. The fastest growing modes favour scales of some 100 m, a tiny fraction of  $r$  (Schmit and Tscharnuter, 1995, 1999; Salo et al., 2001; Schmidt et al., 2001), and as a consequence, the saturation mechanism is controlled by nonlinear travelling waves (Schmidt and Salo, 2003; Latter and Ogilvie, 2009, 2010; Rein and Latter, 2013). It is generally accepted that the fine-scale axisymmetric density waves in Saturn’s A and B-rings are generated and sustained by viscous overstability (Thomson et al., 2007; Colwell et al., 2007; Hedman et al., 2014).

Viscous overstability can generate large-scale features, such as eccentric modes (Borderies et al., 1985; Papaloizou and Lin, 1988; Longaretti and Rappaport, 1995). It is likely that the structure of eccentric ringlets and the outer B-ring edge are partly sculpted by this process (Spitale and Porco, 2010; Nicholson et al., 2014). Similarly, certain gaseous accretion disks may have obtained their eccentricity in this way (Lyubarskij et al., 1994; Ogilvie, 2001; Latter and Ogilvie, 2006b), though the issue is far less clear cut than in the planetary ring context.

One reason why the onset of viscous overstability is problematic in gaseous accretion disks, as opposed to planetary rings, concerns the nature of the viscous stresses. In gaseous disks these are presumed to be supplied by hydrodynamic (or magnetohydrodynamic) turbulence — but it is unclear if

the turbulence responds in the desired way when a density wave propagates through the disk. The stress may not be enhanced in high density-wave crests, and even if it is enhanced the stress may be out of phase with the dynamical oscillation (Ogilvie, 2003). In either case, viscous overstability may fail to occur. Note that the collisional stress in dense planetary rings does not suffer from this shortcoming (Araki and Tremaine, 1986; Salo et al., 2001; Latter and Ogilvie, 2008).

### 1.8.3 Viscous instability

The viscous instability (also called the ‘inflow instability’) occurs when the stresses in a disk decrease with increasing surface density. The equation for small perturbations in the surface density becomes, as a result, a diffusion equation with a negative diffusivity. Physically, a localised bump of density accretes less vigorously than its surroundings and mass piles up at its outer edge, enhancing the overdensity.

In the early 1970s the viscous instability was shown to afflict certain disk models of X-ray binaries, in particular when the disk is assumed optically thick and its stresses proportional to the radiation pressure (Lightman and Eardley, 1974; Shakura and Sunyaev, 1976). But there has always been a question mark regarding the applicability of viscous instability to real accretion disks because of the last assumption. It is by no means assured that the turbulent stresses in radiatively dominated accretion flows behave in the way required (but see Hirose et al., 2009).

Inspired by the *Voyager* images, early theories of planetary ring structure appealed to the viscous instability (Ward, 1981; Lukkari, 1981; Lin and Bodenheimer, 1981), but again doubts were raised about the properties of the viscous stress, and interest dwindled. Kinetic theory indicates that dilute rings possess a stress that decreases with surface density (Goldreich and Tremaine, 1978b; Shu and Stewart, 1985) but also that dense rings emphatically do not (Araki and Tremaine, 1986). If viscous instability is to occur in dense rings, it must attack only the smallest particles selectively (Salo and Schmidt, 2010).

### 1.8.4 Thermal instability and ‘phase’ changes

Gaseous accretion disks may fall into one of many thermal/ionisation equilibria for a given set of parameters. Not all of these are thermally stable and so it is possible that a disk cycles between different states over time, generating quasi-periodic variability in accretion luminosity and non-thermal emission.

The classic and best understood examples are dwarf novae which straddle the temperature threshold for hydrogen ionisation (about 5000 K). Because the opacity increases dramatically in the partially ionised phase, the gas’s cooling rate is a complicated function of the temperature and permits the disk to support three possible thermal equilibria for a given surface density (Meyer and Meyer-Hofmeister, 1981; Faulkner et al., 1983). In the phase space of surface density and temperature, disk equilibria sketch out a characteristic ‘S-curve’, an example of which we plot in Figure 1.13.

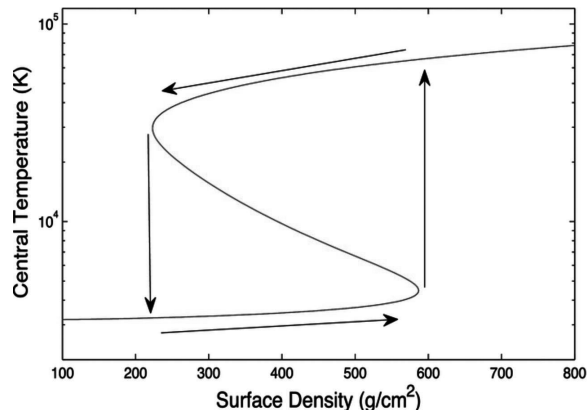


**Figure 1.13** A characteristic dwarf nova S-curve, describing thermal equilibria in the phase space of surface density and temperature. The arrows indicate a limit cycle that the disk may follow. Credit: Latter and Papaloizou (2012).

The disk may then enter a limit cycle, oscillating between the hot, well-ionised, and luminous high state (an outburst) and the cool, poorly ionised, and dim low state. The transition between the two states takes place via thermal fronts that rapidly sweep through the disk. The story is complicated by a raft of ancillary physics, but in general the contact with observations is relatively good. Similar physics is shared with low-mass X-ray binaries, but these systems are not so well understood and the model enjoys less success (Lasota, 2001).

Disks dominated by radiation pressure can support a variety of interesting equilibria partly because of the relative inefficiency of cooling in very hot plasma. In addition to the standard thin disk solution of Shakura and Sunyaev (1973), there exist ‘slim’ and ‘thick’ disks in which radiative cooling is supplanted by radial advection of energy by the gas (Abramowicz et al., 1988). The most extreme case is the advection-dominated accretion flow (ADAF) where little of the dissipated energy is radiated locally and the rotation profile deviates significantly from Keplerian (Narayan and Yi, 1994). If the turbulent stresses are assumed proportional to the total pressure, these solutions are thermally unstable because the heating depends on temperature to a much greater power than cooling (Shakura and Sunyaev, 1976; Piran, 1978). Even though recent MRI simulations indicate that thermal instability can arise in such disks (Jiang et al., 2013), X-ray observations of strongly accreting black hole systems fail to exhibit unstable or cyclic dynamics on the expected timescales (Gierliński and Done, 2004; Done et al., 2007). Only the exceptionally luminous black hole binary, GRS 1915+105, shows anything like an expected limit cycle driven by thermal instability (Done et al., 2004). In contrast there are abundant observations of other kinds of variability, especially in the spectroscopy, and a panoply of well-defined states exist in the phase space of intensity, hardness, and rms fluctuation (Remillard and McClintock, 2006; Belloni, 2010). To date there is no convincing explanation for the cycling between these phases.

Finally, protoplanetary disks are thought to jump aperiodically between high and low accreting states on a time scale of 100+ years. This outbursting behaviour is exemplified by the archetype FU Orionis, though other classes may exist, notably the shorter timescale EXors (Audard et al., 2014). The current theoretical paradigm posits that the low state corresponds to a disk whose central region (the ‘dead zone’) is cold, laminar and inefficiently accreting and that the high state corresponds to one in which this region is engulfed in MRI turbulence. The build-up of mass at the outer edge of the dead zone and a consequent gravitational instability are the trigger for an outburst (Gammie, 1996; Armitage et al., 2001).

Saturn’s rings also exhibit multiple phases. In the inner B-ring there exist adjacent flat and undulatory states, while the middle and outer B-ring breaks up into disjunct bands of intermediate and high optical depth; both phenomena occur on scales of order 100 km (Colwell et al., 2009). In accretion disks the different phases are distributed over time, but in planetary rings, with their achingly slow timescales, adjoining states are distributed spatially. For example, during a dwarf nova outburst the high state overwhelms the disk in  $\sim 1$  day; in contrast, the undulatory state in the inner B-ring may take over the entire ring in  $10^{10}$  days (Latter et al., 2012a).

The origin of the observed states in planetary rings is not well understood. It is perhaps unlikely that they issue from a bistability in the thermal equilibrium itself (as in dwarf novae). For a constant coefficient of restitution  $\epsilon$ , there is only ever one equilibrium for a given set of parameters (Araki and Tremaine, 1986), while experimentally derived laws describing  $\epsilon$ ’s dependence on impact speed yield the same result (Wisdom and Tremaine, 1988; Salo, 1991; Latter and Ogilvie, 2008). Note, however, that if  $\epsilon$  is a non-monotonic function of impact speed then bistability could be possible. Such a coefficient of restitution may correspond to collision models that incorporate particle sticking at low impact speeds (Albers and Spahn, 2006b).

The undulatory and flat states in the inner B-ring could be competing outcomes of the ballistic transport instability (Durisen, 1995), whose nonlinear dynamics supports bistability (Latter et al., 2014a,b). The 100 km structures deeper in the B-ring are more mysterious. Tremaine (2003) proposed that these correspond to shearing and shear-free regions, the latter held together by strong inter-particle adhesion. While it may be possible to hold together 100 km shear-free bands if the disk were restricted to the orbital plane, in three-dimensions the rings’ tensile strength will be too weak because the rings can vertically ‘relax’.

## 1.9 SATELLITE–DISK INTERACTIONS

### 1.9.1 Introduction

Astrophysical bodies that are surrounded by continuous disks often possess discrete satellites as well. Examples include the moons of giant planets, which then interact with

their planetary rings, protoplanets interacting with a circumstellar disk, and binary stars and black holes interacting with accretion disks. Various geometrical configurations are possible, as a satellite can orbit fully interior or exterior to the disk, be confined within an annular gap, or be fully embedded in the disk.

The gravitational interaction between an orbital companion and a disk is a problem of general interest in astrophysics. By generating waves and other disturbances in the disk, the satellite both undergoes orbital evolution and influences disk properties. In addition, observations of the structures induced in the disk can be used to constrain physical properties of both the disk and the perturber.

One important application, discussed in greater detail below, is to planets formed in a gaseous disk around a young star. The planet–disk interaction causes the planet to migrate radially through the disk, a process that needs to be understood and quantified in order to interpret the observed properties and architectures of exoplanetary systems (as well as the Solar System). Ever since the first planets were discovered on orbits very close to solar-type stars, it was suggested that planetary migration brought them to their current locations (Mayor and Queloz, 1995). As more and more hot Jupiters have been found, it is generally accepted that these planets formed at locations beyond 1 AU and have since migrated inwards.

Orbital migration can also be important in AGN. When two galaxies merge, the central black hole of the smaller galaxy interacts with the accretion disk surrounding the larger black hole, in a way analogous to a planet interacting with a circumstellar disk. Inward orbital migration leads eventually to a compact binary black hole that merges as a result of gravitational radiation, as spectacularly confirmed by recent observations (Abbott et al., 2016).

Finally, many of the observed structures in astrophysical disks and planetary rings can be attributed to satellite–disk interactions. Examples include the Cassini division, the Encke and Keeler gaps, the spiral waves in Saturn’s rings, as well as the spiral arms in interacting galaxies and the tidal truncation of accretion disks in binary stars. Planet–disk interaction can also create annular gaps and spiral structures in PP disks, some examples of which may have been recently observed (see section 1.2.1).

### 1.9.2 Wave launching, coorbital torques and type-I migration

The simplest situation involves a satellite on a circular orbit that is coplanar with the disk. The satellite exerts a periodic gravitational force on the disk and excites its epicyclic motion. The forced motion is resonant at a series of radii, located both interior and exterior to the satellite’s orbit, and the disk responds by launching a spiral density wave at each of these resonances. To the extent that the epicyclic frequency corresponds to the orbital frequency, these Lindblad resonances can be identified with mean-motion resonances involving commensurabilities of the form  $m : m \pm 1$  between the orbital frequencies of the satellite and the disk; in fact they are slightly shifted radially because of small departures

from Keplerian motion due to pressure gradients, disk self-gravity, oblateness of the central body, etc.

The act of launching a wave involves a transfer of energy and angular momentum from the satellite's orbit. As the waves propagate radially away from the Lindblad resonances, their radial wavelength decreases and they are damped by viscosity or other dissipative processes. The damping may be enhanced if the waves attain nonlinear amplitudes. The angular-momentum flux carried by the wave is transferred to the disk as the wave is damped and thus a resonant torque is exerted between the satellite and the disk.

Numerous examples of these density waves in Saturn's A-ring were observed by the *Voyager* and *Cassini* spacecraft, and have been identified with specific Lindblad resonances with various moons that orbit outside the A-ring. A different type of density wave is seen near the edges of the Encke and Keeler gaps in the outer A-ring. These are excited by the satellites that orbit within these gaps and are therefore closer to the ring material than the larger external moons. In these cases the wake cannot be identified with a single Lindblad resonance, although it can be thought of as a superposition of waves generated at many such resonances of high order.

In the case of planets interacting with PP disks, related phenomena have manifested chiefly in theoretical work (although there is now some observational evidence of spiral waves in PP disks, which can be explained best by embedded planets; Dong et al., 2015, 2016), and in recent years hydrodynamic simulations have led the way in determining the nonlinear dynamics of planet-disk interactions. Embedded satellites that are not massive enough to open a gap in the disk's density profile undergo what is called *type-I migration* (Goldreich and Tremaine, 1978a, 1980; Ward, 1997). The density waves launched at different Lindblad resonances constructively interfere to produce a coherent one-armed spiral wake (Ogilvie and Lubow, 2002), a narrow overdense region. The wake is not symmetric about the satellite's location, because of the circular geometry and possible radial gradients in the properties of the unperturbed disk. The satellite therefore experiences a net gravitational torque, which under most circumstances is negative, leading to inward migration of the satellite. A snapshot of the surface density in a hydrodynamic disk simulation with an embedded planet of 10 Earth masses is shown in Figure 1.14

This description is incomplete because a different type of interaction happens closer to the satellite's orbit, where disk material approximately corotates with the satellite. In this region the relative motion of the disk and satellite is too slow for density waves to be excited, but the satellite can instead generate non-wavelike disturbances in the potential vorticity and entropy of the disk, each of which involves an asymmetric rearrangement of the surface density and therefore a torque. In distinction to the Lindblad torques associated with the launching of density waves, the torques arising from this region are known as coorbital, corotation or horseshoe torques. The last name comes from the property that, in the frame rotating with the satellite's orbit, disk material in the coorbital region has streamlines that librate rather



**Figure 1.14** Hydrodynamic simulation of a planet of 10 Earth masses undergoing type-I migration in a protoplanetary disk. The surface density is plotted in grey-scale.

than circulate, and involve horseshoe-shaped turns near the satellite's longitude.

The entropy-related corotation torque can lead to stalling of planets exceeding roughly 3-5 earth masses at specific disk locations that vary with time (Baruteau et al., 2014). Ultimately, however, these torques are sustained by dissipative effects, such as viscosity, thermal diffusivity, and radiative cooling which are all uncertain (Paardekooper and Papaloizou, 2008, 2009). In addition, the physics of the coorbital region is strongly nonlinear, and thus difficult to describe accurately. The net (Lindblad plus coorbital) torque is subject to similar uncertainties.

Nevertheless, there is general agreement that planets of Earth mass typically migrate towards the star on a timescale of a few hundred thousand years. This poses a problem for planet formation because the viscous timescale, i.e. the lifetime of the accretion disk, is thought to be significantly longer than that. The inconvenient conclusion is that every Earth-mass planet in a protoplanetary disk should have migrated into the star. Various ways to prevent this from happening have been proposed. These ideas include the stochastic torques arising from turbulence in the disk (see later), positive torques associated with asymmetric heating in the planet's neighbourhood (Benítez-Llambay et al., 2015), and so-called *planet traps* due to dead zones, snow lines or other features in the disk (Masset et al., 2006). Similar physics may also control the migration of propellers in Saturn's rings (Tiscareno, 2013). We still, however, lack a general theory capable of predicting the speed and direction of type-I migration, which is vitally needed to link together the early and late stages of planet formation.



### 1.9.3 Gap opening and type-II migration

In the type-I regime, while the fractional surface density perturbation in the wake can become of order unity at some distances from the satellite (involving a shock, in the case of a gas disk), the azimuthally averaged surface density of the disk is not significantly perturbed. More massive satellites, however, are able to deplete the disk locally by opening an annular gap. This happens because the Lindblad torques exerted by the satellite on the interior and exterior parts of the disk are negative and positive, respectively, causing both to recede from the satellite's orbit.

The scaling laws for gap opening have been formulated by Lin and Papaloizou (1986, 1993). Note that it is difficult to quantify the process exactly because gaps can be of differing degrees of cleanliness. In order to open a gap, the mass ratio  $M_s/M$  of the satellite and the central object should be sufficiently large. A first criterion is that  $M_s/M \gtrsim (H/r)^3$ , or, equivalently, that the Hill radius  $R_H \gtrsim H$ . This is the condition for the disturbance generated in the disk to be nonlinear close to the satellite, which allows it to be dissipated locally. A second criterion, which is usually more stringent, is that  $M_s/M \gtrsim (81\pi/8)(\nu/r^2\Omega)$ . This is the condition that the tidal torque exceed the viscous torque in the undisturbed disk (if indeed it can be adequately described by a simple kinematic viscosity). When applied to a protoplanetary disk, the latter criterion implies that a planet of about Saturn's mass or greater is able to open a gap. When applied to the outer part of Saturn's A-ring, the criteria imply that a moon of about Daphnis's mass or greater is able to open a gap.

The characteristics of satellite migration change significantly when a gap opens — a situation referred to as *type-II migration* (Figure 1.15). The gap effectively divides the disk into interior and exterior disks, making it difficult (or impossible) for material to pass through. The satellite is effectively locked to the viscous evolution of the disk, and may even retard that evolution if it is more massive than the interior disk. The timescales of type-II migration are therefore in general longer than those of type-I migration. HL Tau (see Figure 1.1) might be a system where planets were able to open gaps, although confirmation of this interpretation is still pending.

### 1.9.4 Stochastic migration

Classical theories of type-I and type-II migration assume a smooth, laminar disk as a background state. Since disks are typically active with a number of instabilities, this may be a poor approximation. Instabilities can lead to turbulence and cause density perturbations on many scales. This can, especially for small embedded satellites, lead to migration that resembles a random walk in the orbital parameters (Nelson and Papaloizou, 2004; Rein and Papaloizou, 2009). This *stochastic migration* is relevant for low-mass planets in PP disks in the presence of the MRI or GI, and for moonlets in planetary rings (discussed in detail in the Spahn chapter). If the moonlets are small enough, their migration will be dominated by the stochastic component (Rein and Papaloizou,

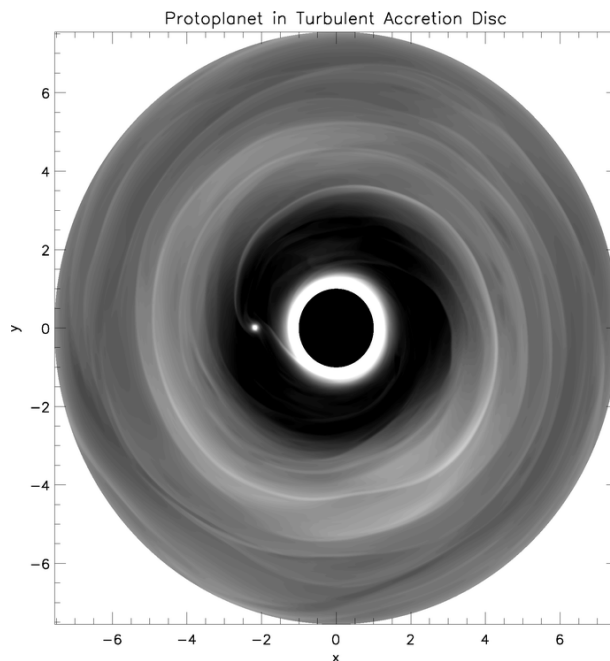


**Figure 1.15** Hydrodynamic simulation of a planet of 5 Jupiter masses opening a gap and undergoing type-II migration in a turbulent protoplanetary disk. Again the surface density is plotted. Credit: Nelson & Papaloizou (2003).

2010), rather than the classical type-I torque. The main contributions to the stochastic migration of moonlets in rings are collisions with ring particles (which have no analogue in PP disks) and interactions with the (temporary) clumps and overdensities created predominantly by self-gravity wakes.

### 1.9.5 Tidal truncation and disk edges

Satellites that are significantly more massive than those that are able to open a gap can truncate a disk at great distance. In Saturn's rings the outer edge of the B-ring is associated with the 2:1 Lindblad resonance with Mimas, while the outer edge of the A-ring coincides with the 7:6 resonance with the coorbital moons Janus and Epimetheus. Related phenomena occur in accretion disks in binary stars; for typical mass ratios, however, the 2:1 resonance is so strong that the disk is truncated well inside it (Papaloizou and Pringle, 1977; Paczynski, 1977). On the other hand, the  $\epsilon$ -ring of Uranus appears to be 'shepherded', i.e. radially confined, by the satellites Cordelia and Ophelia on either side, via discrete Lindblad resonances (Goldreich and Porco, 1987b).

In order to explain the extreme sharpness of the edges of planetary rings, in particular those mentioned above, it has been found necessary to appeal to a modification of the viscous torque that occurs when the ring carries a nonlinear density wave (Borderies et al., 1982, 1989, Chapters by Longaretti and Nicholson). The presence of the wave alters the velocity gradient associated with circular orbits in such a way that the angular-momentum flux is reduced to zero when the wave has a critical amplitude, and is reversed for waves of higher amplitude. Without this effect, the edges of planetary rings would be smoothed out by viscosity and

it would be difficult or impossible to account for the shepherding process. It is not known whether the modification or reversal of the angular-momentum flux plays a role in gaseous disks.

### 1.9.6 Eccentricity and inclination

If the satellite’s orbit is eccentric or inclined with respect to the disk, then the gravitational force on the disk contains additional components that launch density or bending waves at Lindblad or vertical resonances. The eccentricity or inclination of the satellite evolves as a result of these interactions. For satellites embedded in the disk, a small ( $\lesssim H/r$ ) eccentricity  $e$  or inclination  $i$  is damped on a timescale that is shorter than that for type-I migration. This interaction is dominated by disk material close to the planet. For larger  $e$  or  $i$  the damping is less efficient and the direction and rate of migration may also be affected. When the planet’s speed relative to the local gas exceeds the sound speed or velocity dispersion (as happens for example when the inclination of the satellite brings it above the disk, i.e.  $i \gtrsim H/r$ ) the interaction is dominated by gas drag similar to that of a star passing through the interstellar medium (Rein, 2012).

More massive satellites that are well separated from the disk material interact through more distant orbital resonances and the net effect can, under some circumstances, be a growth in  $e$  and/or  $i$  (Goldreich and Tremaine, 1981; Borderies et al., 1983, 1984). In fact, the disk can also become elliptical and/or warped through these interactions, and the relative magnitude of the  $e$  or  $i$  of the disk and the satellite depends on their coupled dynamics (Lubow and Ogilvie, 2001; Teyssandier and Ogilvie, 2016).

A good example of satellite–disk interaction producing a growth of eccentricity occurs in SU Ursae Majoris binary stars, where the accretion disk around a white dwarf is understood to become elliptical as a result of an interaction with the companion star at the 3:1 orbital resonance, an example of an eccentric Lindblad resonance (Lubow, 1991). This is the ‘superhump’ phenomenon, so called because of the associated modulation of the light curve during a super-outburst.

A similar process may be responsible for maintaining the eccentricity of Uranus’s  $\epsilon$ -ring; the 47:49 eccentric Lindblad resonance with its inner ‘shepherd’ satellite, Cordelia, lies within the ring (Goldreich and Porco, 1987b). However, it should be noted that other narrow rings around Saturn and Uranus are also found to be eccentric even though they have no observed shepherds (see Nicholson chapter).

## 1.10 CONCLUSION

In this chapter we make explicit connections between the study of planetary rings and of other astrophysical disks, putting an emphasis on dynamics. Disk systems exhibit an enormous physical and dynamical diversity, but one anchored upon the fundamental balance between radial gravity and the centrifugal force. A relic of formation, their or-

bit angular momentum is inherited from the collapse of a cloud, the disruption of body by a massive companion, or the collision of two bodies around a more massive object. This ‘excess’ angular momentum thwarts the simple accretion of disk material upon the central body, irrespective of the different formation routes, and leads to planetary rings and astrophysical disks.

Through the diversity of composition and physics one can discern recurrent themes. To begin, most gaseous disks support hydrodynamical (or magnetohydrodynamical) activity that permits disk material to slowly shed or redistribute its angular momentum and thus ultimately accrete. By liberating orbital energy this activity also causes the disk to radiate — the key to understanding certain high energy sources. The outward transport of angular momentum (whether mediated by turbulent motions in gas or collisions between particles) controls the evolution and lifetime of the disk or ring. Though the ‘viscous’ lifespans of planetary rings and gaseous disks differ by orders of magnitude, accretion represents one of their key connections.

Collisional dynamics presents a link between rings and other particulate disks, such as debris disks and the belts of dust and planetesimals orbiting young stars. In the ring context, collisions not only help transport angular momentum but also control the composition, structure, and size evolution of the constituent particles themselves. The same processes govern PP and debris disks, leading to the formation of planetesimals and planets in the former, and dust in the latter.

Both rings and disks support the passage of waves and the growth of instabilities, which contribute to the activity required to sustain accretion and angular-momentum transport. Regarding self-excited instabilities, only in the case of gravitational instability is (nearly) the same process reliably occurring in both rings and gaseous disks, although viscous overstability may be a second example. Satellite–disk interactions, on the other hand, provide the richest set of dynamics shared by the two classes of systems. Spiral density waves, gap formation, and satellite migration, all now directly observed in detail around Saturn, have important analogues around young stars that are beginning to yield observational manifestations (with instruments such as ALMA). In that respect, observations of satellite–disk interactions in planetary rings are ahead of those in PP disks by a few decades. But just as the Voyager data proved so exciting and fruitful during the 1980s, so should ALMA observations in the following decade, as its full capabilities are brought to bear on the problem of exoplanets and their host disks.

Given these overlaps, it is no surprise the fields of disks and of rings have connected in mutually beneficial ways. The clearest instance is in the study of satellite–disk interactions, where work on binary stars and Saturn’s rings converged fruitfully in the theoretical understanding of planet–disk coupling in the 1980s. Another example is the research in disk instabilities, first introduced in gaseous disks in the 1970s but matured in the planetary ring context over the next few decades. Despite this historically close connection, there yet remain a number of correspondences that have yet

to be fully capitalised upon and which form the basis for several appealing research directions.

The size-distribution dynamics of dense rings is an underdeveloped area compared with that for debris disks and planet formation. Though arguably a more difficult problem, the techniques and tools of the latter could be profitably adapted to help explain the distributions in Saturn’s rings, which are observationally well constrained in comparison to those more distant particulate systems. Note that the statistical approaches used in debris disks may be applied without too much complication to the F-ring, as it is probably the closest ring analogue. On the other hand, this is also an opportunity to determine how well these techniques and tools perform on an object so much better constrained than a debris disk. An especially compelling sub-question is the provenance of the propellers in the A-ring. Is it possible that these large objects are related to the ‘lucky’ planetesimals that grow to large sizes in PP disks, their smaller brethren languishing in the cm to m size classes?

Another area of fruitful overlap is in the detailed microphysics of collisions. Only recently have studies of dense planetary rings moved away from the bouncing hard-sphere model of ring particles. In contrast, the numerical treatment of collisions in planet formation is much better developed, allowing for the full gamut of physical processes (compaction, mass transfer, fragmentation, reaccretion, etc.). Is it possible to establish clear barriers to growth in dense rings, as in PP disks? Can we construct a typology of collisional outcomes in dense rings as clearly as in planetesimal belts?

Gravitational instability (and gravitoturbulence) is shared by planetary rings, PP disks, and galactic disks. However, the details of its onset and saturation are still unclear in each context. A more unified approach would nail down its manifestation in all three classes, and indeed uncover more profound connections with other subcritical transitions to turbulence in shearing and rotating systems. Another area worth exploring is the production of tidal streams around white dwarfs, which clearly shares the same physics of certain ring formation scenarios, especially of narrow rings. Finally, the field of satellite–disk interactions, though mature, could but undoubtedly support further connections between rings and disks. As observations of PP disks become more and more detailed due to ALMA, the intricate and varied morphologies supported by Saturn’s rings will provide valuable analogues with which to understand them.

## Acknowledgments

The authors thank the anonymous reviewer and the editors Matthew Tiscareno and Carl Murray for a set of helpful comments. They are particularly indebted to the generosity of colleagues and friends who read through earlier stages of the manuscript, in particular Julia Forman, Cleo Loi, Pierre-Yves Longaretti, John Papaloizou, and Mark Wyatt. The chapter was much improved by their insightful and helpful remarks. We also thank Tobias Heinemann and Antoine Riols-Fonclare for providing figures.

## REFERENCES

- Abbott, B. P., Abbott, R., Abbott, T. D., Abernathy, M. R., Acernese, F., Ackley, K., Adams, C., Adams, T., Addesso, P., Adhikari, R. X., and et al. 2016. Observation of Gravitational Waves from a Binary Black Hole Merger. *Physical Review Letters*, **116**(6), 061102.
- Abramowicz, M. A., and Fragile, P. C. 2013. Foundations of Black Hole Accretion Disk Theory. *Living Reviews in Relativity*, **16**.
- Abramowicz, M. A., Czerny, B., Lasota, J. P., and Szuszkiewicz, E. 1988. Slim accretion disks. *ApJ*, **332**, 646–658.
- Albers, N., and Spahn, F. 2006a. The influence of particle adhesion on the stability of agglomerates in Saturn’s rings. *Icarus*, **181**, 292–301.
- Albers, N., and Spahn, F. 2006b. The influence of particle adhesion on the stability of agglomerates in Saturn’s rings. *Icarus*, **181**, 292–301.
- Alexander, R. D., Clarke, C. J., and Pringle, J. E. 2006. Photoevaporation of protoplanetary discs - II. Evolutionary models and observable properties. *MNRAS*, **369**, 229–239.
- ALMA Partnership, Brogan, C. L., Pérez, L. M., Hunter, T. R., Dent, W. R. F., Hales, A. S., Hills, R. E., Corder, S., Fomalont, E. B., Vlahakis, C., Asaki, Y., Barkats, D., Hirota, A., Hodge, J. A., Impellizzeri, C. M. V., Kneissl, R., Liuzzo, E., Lucas, R., Marcelino, N., Matsushita, S., Nakanishi, K., Phillips, N., Richards, A. M. S., Toledo, I., Aladro, R., Brogiere, D., Cortes, J. R., Cortes, P. C., Espada, D., Galarza, F., Garcia-Appadoo, D., Guzman-Ramirez, L., Humphreys, E. M., Jung, T., Kameno, S., Laing, R. A., Leon, S., Marconi, G., Mignano, A., Nikolic, B., Nyman, L.-A., Radiszcz, M., Remijan, A., Rodón, J. A., Sawada, T., Takahashi, S., Tilanus, R. P. J., Vila Vilaro, B., Watson, L. C., Wiklind, T., Akiyama, E., Chapillon, E., de Gregorio-Monsalvo, I., Di Francesco, J., Gueth, F., Kawamura, A., Lee, C.-F., Nguyen Luong, Q., Mangum, J., Pietu, V., Sanhueza, P., Saigo, K., Takakuwa, S., Ubach, C., van Kempen, T., Wootten, A., Castro-Carrizo, A., Francke, H., Gallardo, J., Garcia, J., Gonzalez, S., Hill, T., Kaminski, T., Kurono, Y., Liu, H.-Y., Lopez, C., Morales, F., Plarre, K., Schieven, G., Testi, L., Videla, L., Villard, E., Andreani, P., Hibbard, J. E., and Tatematsu, K. 2015. The 2014 ALMA Long Baseline Campaign: First Results from High Angular Resolution Observations toward the HL Tau Region. *ApJL*, **808**, L3.
- Andrews, S. M., Wilner, D. J., Espaillat, C., Hughes, A. M., Dullemond, C. P., McClure, M. K., Qi, C., and Brown, J. M. 2011. Resolved Images of Large Cavities in Protoplanetary Transition Disks. *ApJ*, **732**, 42.
- Antonucci, R. 1993. Unified models for active galactic nuclei and quasars. *ARAA*, **31**, 473–521.
- Araki, S., and Tremaine, S. 1986. The dynamics of dense particle disks. *Icarus*, **65**, 83–109.
- Armitage, P. J. 2011. Dynamics of Protoplanetary Disks. *ARAA*, **49**, 195–236.
- Armitage, P. J., Livio, M., and Pringle, J. E. 2001. Episodic accretion in magnetically layered protoplanetary discs. *MNRAS*, **324**, 705–711.
- Attree, N. O., Murray, C. D., Cooper, N. J., and Williams, G. A. 2012. Detection of Low-velocity Collisions in Saturn’s F Ring. *ApJL*, **755**, L27.
- Attree, N. O., Murray, C. D., Williams, G. A., and Cooper, N. J. 2014. A survey of low-velocity collisional features in Saturn’s F ring. *Icarus*, **227**, 56–66.
- Audard, M., Ábrahám, P., Dunham, M. M., Green, J. D., Grosso, N., Hamaguchi, K., Kastner, J. H., Kóspál, Á., Lodato, G., Romanova, M. M., Skinner, S. L., Vorobyov, E. I., and Zhu, Z. 2014. Episodic Accretion in Young Stars. *Protostars and Planets VI*, 387–410.
- Aumann, H. H., Beichman, C. A., Gillett, F. C., de Jong, T., Houck, J. R., Low, F. J., Neugebauer, G., Walker, R. G., and Wesselius, P. R. 1984. Discovery of a shell around Alpha Lyrae. *ApJL*, **278**, L23–L27.
- Baade, W., and Minkowski, R. 1954. Identification of the Radio Sources in Cassiopeia, Cygnus A, and Puppis A. *ApJ*, **119**, 206.
- Backman, D. E., and Paresce, F. 1993. Main-sequence stars with circumstellar solid material - The VEGA phenomenon. Pages 1253–1304 of: Levy, E. H., and Lunine, J. I. (eds), *Protostars and Planets III*.
- Balbus, S. A., and Hawley, J. F. 1991. A powerful local shear instability in weakly magnetized disks. I - Linear analysis. II - Nonlinear evolution. *ApJ*, **376**, 214–233.
- Balbus, S. A., and Hawley, J. F. 1998. Instability, turbulence, and enhanced transport in accretion disks. *Reviews of Modern Physics*, **70**, 1–53.
- Balbus, S. A., and Papaloizou, J. C. B. 1999. On the Dynamical Foundations of  $\alpha$  Disks. *ApJ*, **521**, 650–658.
- Barbara, J. M., and Esposito, L. W. 2002. Moonlet Collisions and the Effects of Tidally Modified Accretion in Saturn’s F Ring. *Icarus*, **160**, 161–171.
- Barge, P., and Sommeria, J. 1995. Did planet formation begin inside persistent gaseous vortices? *A&A*, **295**, L1–L4.
- Barker, A. J., and Latter, H. N. 2015. On the vertical-shear instability in astrophysical discs. *MNRAS*, **450**(June), 21–37.
- Baruteau, C., Crida, A., Paardekooper, S.-J., Masset, F., Guilet, J., Bitsch, B., Nelson, R., Kley, W., and Papaloizou, J. 2014. Planet-Disk Interactions and Early Evolution of Planetary Systems. *Protostars and Planets VI*, 667–689.
- Bell, K. R., and Lin, D. N. C. 1994. Using FU Orionis outbursts to constrain self-regulated protostellar disk models. *ApJ*, **427**, 987–1004.

- Belloni, T. M. 2010. States and Transitions in Black Hole Binaries. Page 53 of: Belloni, T. (ed), *Lecture Notes in Physics, Berlin Springer Verlag*. Lecture Notes in Physics, Berlin Springer Verlag, vol. 794.
- Benisty, M., Juhasz, A., Boccaletti, A., Avenhaus, H., Milli, J., Thalmann, C., Dominik, C., Pinilla, P., Buenzli, E., Pohl, A., Beuzit, J.-L., Birnstiel, T., de Boer, J., Bonnefoy, M., Chauvin, G., Christiaens, V., Garufi, A., Grady, C., Henning, T., Huelamo, N., Isella, A., Langlois, M., Ménard, F., Mouillet, D., Olofsson, J., Pantin, E., Pinte, C., and Pueyo, L. 2015. Asymmetric features in the protoplanetary disk MWC 758. *A&A*, **578**, L6.
- Benítez-Llambay, P., Masset, F., Koenigsberger, G., and Szulágyi, J. 2015. Planet heating prevents inward migration of planetary cores. *Nature*, **520**(Apr.), 63–65.
- Beurle, K., Murray, C. D., Williams, G. A., Evans, M. W., Cooper, N. J., and Agnor, C. B. 2010. Direct Evidence for Gravitational Instability and Moonlet Formation in Saturn’s Rings. *ApJL*, **718**, L176–L180.
- Binney, J., and Merrifield, M. 1998. *Galactic Astronomy*.
- Binney, J., and Tremaine, S. 2008. *Galactic Dynamics: Second Edition*. Princeton University Press.
- Biretta, J. A., Sparks, W. B., and Macchetto, F. 1999. Hubble Space Telescope Observations of Superluminal Motion in the M87 Jet. *ApJ*, **520**, 621–626.
- Blaes, O. M., and Balbus, S. A. 1994. Local shear instabilities in weakly ionized, weakly magnetized disks. *ApJ*, **421**, 163–177.
- Blandford, R. D., and Payne, D. G. 1982. Hydromagnetic flows from accretion discs and the production of radio jets. *MNRAS*, **199**, 883–903.
- Bloom, J. S., Giannios, D., Metzger, B. D., Cenko, S. B., Perley, D. A., Butler, N. R., Tanvir, N. R., Levan, A. J., O’Brien, P. T., Strubbe, L. E., De Colle, F., Ramirez-Ruiz, E., Lee, W. H., Nayakshin, S., Quataert, E., King, A. R., Cucchiara, A., Guillochon, J., Bower, G. C., Fruchter, A. S., Morgan, A. N., and van der Horst, A. J. 2011. A Possible Relativistic Jetted Outburst from a Massive Black Hole Fed by a Tidally Disrupted Star. *Science*, **333**, 203–.
- Blum, J., and Wurm, G. 2008. The Growth Mechanisms of Macroscopic Bodies in Protoplanetary Disks. *ARAA*, **46**, 21–56.
- Blumenthal, G. R., Lin, D. N. C., and Yang, L. T. 1984. On the overstability of axisymmetric oscillations in thin accretion disks. *ApJ*, **287**, 774–784.
- Bodrova, A., Schmidt, J., Spahn, F., and Brilliantov, N. 2012. Adhesion and collisional release of particles in dense planetary rings. *Icarus*, **218**, 60–68.
- Bonsor, A., and Wyatt, M. 2010. Post-main-sequence evolution of A star debris discs. *MNRAS*, **409**, 1631–1646.
- Bonsor, A., Mustill, A. J., and Wyatt, M. C. 2011. Dynamical effects of stellar mass-loss on a Kuiper-like belt. *MNRAS*, **414**, 930–939.
- Borderies, N., Goldreich, P., and Tremaine, S. 1982. Sharp edges of planetary rings. *Nature*, **299**(Sept.), 209–211.
- Borderies, N., Goldreich, P., and Tremaine, S. 1983. The dynamics of elliptical rings. *AJ*, **88**(Oct.), 1560–1568.
- Borderies, N., Goldreich, P., and Tremaine, S. 1984. Excitation of inclinations in ring-satellite systems. *ApJ*, **284**(Sept.), 429–434.
- Borderies, N., Goldreich, P., and Tremaine, S. 1985. A granular flow model for dense planetary rings. *Icarus*, **63**, 406–420.
- Borderies, N., Goldreich, P., and Tremaine, S. 1989. The formation of sharp edges in planetary rings by nearby satellites. *Icarus*, **80**(Aug.), 344–360.
- Boss, A. P. 1998. Evolution of the Solar Nebula. IV. Giant Gaseous Protoplanet Formation. *ApJ*, **503**, 923–937.
- Boss, A. P., and Graham, J. A. 1993. Clumpy disk accretion and chondrule formation. *Icarus*, **106**, 168.
- Braginskii, S. I. 1965. Transport Processes in a Plasma. *Reviews of Plasma Physics*, **1**, 205.
- Brauer, F., Dullemond, C. P., and Henning, T. 2008. Coagulation, fragmentation and radial motion of solid particles in protoplanetary disks. *A&A*, **480**, 859–877.
- Bridges, F. G., Hatzes, A., and Lin, D. N. C. 1984. Structure, stability and evolution of Saturn’s rings. *Nature*, **309**, 333–335.
- Brilliantov, N., Krapivsky, P. L., Bodrova, A., Spahn, F., Hayakawa, H., Stadnichuk, V., and Schmidt, J. 2015. Size distribution of particles in Saturn’s rings from aggregation and fragmentation. *Proceedings of the National Academy of Science*, **112**, 9536–9541.
- Broadfoot, A. L., Herbert, F., Holberg, J. B., Hunten, D. M., Kumar, S., Sandel, B. R., Shemansky, D. E., Smith, G. R., Yelle, R. V., Strobel, D. F., Moos, H. W., Donahue, T. M., Atreya, S. K., Bertaux, J. L., Blamont, J. E., McConnell, J. C., Dessler, A. J., Linick, S., and Springer, R. 1986. Ultraviolet spectrometer observations of Uranus. *Science*, **233**, 74–79.
- Burns, J. A., Lamy, P. L., and Soter, S. 1979. Radiation forces on small particles in the solar system. *Icarus*, **40**, 1–48.
- Burns, J. A., Showalter, M. R., Hamilton, D. P., Nicholson, P. D., de Pater, I., Ockert-Bell, M. E., and Thomas, P. C. 1999. The Formation of Jupiter’s Faint Rings. *Science*, **284**, 1146.
- Burrows, D. N., Kennea, J. A., Ghisellini, G., Mangano, V., Zhang, B., Page, K. L., Eracleous, M., Romano, P., Sakamoto, T., Falcone, A. D., Osborne, J. P., Campana, S., Beardmore, A. P., Breeveld, A. A., Chester, M. M., Corbet, R., Covino, S., Cummings, J. R., D’Avanzo, P., D’Elia, V., Esposito, P., Evans, P. A., Fugazza, D., Gelbord, J. M., Hiroi, K., Holland, S. T., Huang, K. Y., Im, M., Israel, G., Jeon, Y., Jeon, Y.-B., Jun, H. D., Kawai, N., Kim, J. H., Krimm, H. A., Marshall, F. E., P. Mészáros, Negoro, H., Omodei, N., Park, W.-K., Perkins, J. S., Sugizaki, M., Sung, H.-I., Tagliaferri, G., Troja, E., Ueda, Y., Urata, Y., Usui, R., Antonelli, L. A., Barthelmy, S. D., Cusumano, G., Giommi, P., Melandri, A., Perri, M., Racusin, J. L., Sbarufatti, B., Siegel, M. H., and Gehrels, N. 2011. Relativistic jet activity from the tidal disruption of a star by a massive black hole. *Nature*, **476**, 421–424.
- Cameron, A. G. W. 1978. Physics of the primitive solar accretion disk. *Moon and Planets*, **18**, 5–40.
- Camichel, H. 1958. Mesures photométriques de Saturne et de son anneau. *Annales d’Astrophysique*, **21**, 231.
- Cannizzo, J. K., and Mattei, J. A. 1998. A Study of the Outbursts in SS Cygni. *ApJ*, **505**(Sept.), 344–351.
- Canup, R. M. 2010. Origin of Saturn’s rings and inner moons by mass removal from a lost Titan-sized satellite. *Nature*, **468**, 943–946.
- Chandrasekhar, S. 1969. *Ellipsoidal figures of equilibrium*.
- Charles, P. A., and Coe, M. J. 2006. *Optical, ultraviolet and infrared observations of X-ray binaries*. Pages 215–265.
- Charnoz, S., Morbidelli, A., Dones, L., and Salmon, J. 2009. Did Saturn’s rings form during the Late Heavy Bombardment? *Icarus*, **199**, 413–428.
- Clarke, C. J., and Pringle, J. E. 1993. Accretion disc response to a stellar fly-by. *MNRAS*, **261**(Mar.), 190–202.



- Colombo, G., Goldreich, P., and Harris, A. W. 1976. Spiral structure as an explanation for the asymmetric brightness of Saturn's A ring. *Nature*, **264**(Nov.), 344.
- Colwell, J. E., Esposito, L. W., Sremčević, M., Stewart, G. R., and McClintock, W. E. 2007. Self-gravity wakes and radial structure of Saturn's B ring. *Icarus*, **190**, 127–144.
- Colwell, J. E., Nicholson, P. D., Tiscareno, M. S., Murray, C. D., French, R. G., and Marouf, E. A. 2009. *The Structure of Saturn's Rings*. Page 375.
- Cuzzi, J. N., and Burns, J. A. 1988. Charged particle depletion surrounding Saturn's F ring - Evidence for a moonlet belt? *Icarus*, **74**, 284–324.
- Daisaka, H., Tanaka, H., and Ida, S. 2001. Viscosity in a Dense Planetary Ring with Self-Gravitating Particles. *Icarus*, **154**, 296–312.
- Debes, J. H., and Sigurdsson, S. 2002. Are There Unstable Planetary Systems around White Dwarfs? *ApJ*, **572**, 556–565.
- Debes, J. H., Walsh, K. J., and Stark, C. 2012. The Link between Planetary Systems, Dusty White Dwarfs, and Metal-polluted White Dwarfs. *ApJ*, **747**, 148.
- Dohnanyi, J. S. 1969. Collisional Model of Asteroids and Their Debris. *JGR*, **74**(May), 2531–2554.
- Dominik, C., and Decin, G. 2003. Age Dependence of the Vega Phenomenon: Theory. *ApJ*, **598**, 626–635.
- Done, C., Wardziński, G., and Gierliński, M. 2004. GRS 1915+105: the brightest Galactic black hole. *MNRAS*, **349**, 393–403.
- Done, C., Gierliński, M., and Kubota, A. 2007. Modelling the behaviour of accretion flows in X-ray binaries. Everything you always wanted to know about accretion but were afraid to ask. *AARv*, **15**(Dec.), 1–66.
- Dones, L. 1991. A recent cometary origin for Saturn's rings? *Icarus*, **92**, 194–203.
- Dong, R., Zhu, Z., Rafikov, R. R., and Stone, J. M. 2015. Observational Signatures of Planets in Protoplanetary Disks: Spiral Arms Observed in Scattered Light Imaging Can Be Induced by Planets. *ApJL*, **809**(Aug.), L5.
- Dong, R., Zhu, Z., Fung, J., Rafikov, R., Chiang, E., and Wagner, K. 2016. An M Dwarf Companion and Its Induced Spiral Arms in the HD 100453 Protoplanetary Disk. *ApJL*, **816**(Jan.), L12.
- Donley, J. L., Brandt, W. N., Eracleous, M., and Boller, T. 2002. Large-Amplitude X-Ray Outbursts from Galactic Nuclei: A Systematic Survey using ROSAT Archival Data. *AJ*, **124**, 1308–1321.
- Draine, B. T. 2011. *Physics of the Interstellar and Intergalactic Medium*.
- Dullemond, C. P., and Dominik, C. 2005. Dust coagulation in protoplanetary disks: A rapid depletion of small grains. *A&A*, **434**, 971–986.
- Durisen, R. H. 1984. Transport effects due to particle erosion mechanisms. Pages 416–446 of: Greenberg, R., and Brahic, A. (eds), *IAU Colloq. 75: Planetary Rings*.
- Durisen, R. H. 1995. An instability in planetary rings due to ballistic transport. *Icarus*, **115**, 66–85.
- Durisen, R. H., Boss, A. P., Mayer, L., Nelson, A. F., Quinn, T., and Rice, W. K. M. 2007. Gravitational Instabilities in Gaseous Protoplanetary Disks and Implications for Giant Planet Formation. *Protostars and Planets V*, 607–622.
- Eggen, O. J., Lynden-Bell, D., and Sandage, A. R. 1962. Evidence from the motions of old stars that the Galaxy collapsed. *ApJ*, **136**, 748.
- Eiroa, C., Marshall, J. P., Mora, A., Montesinos, B., Absil, O., Augereau, J. C., Bayo, A., Bryden, G., Danchi, W., del Burgo, C., Ertel, S., Fridlund, M., Heras, A. M., Krivov, A. V., Launhardt, R., Liseau, R., Löhne, T., Maldonado, J., Pilbratt, G. L., Roberge, A., Rodmann, J., Sanz-Forcada, J., Solano, E., Stapelfeldt, K., Thébault, P., Wolf, S., Ardila, D., Arévalo, M., Beichmann, C., Faramaz, V., González-García, B. M., Gutiérrez, R., Lebreton, J., Martínez-Arnáiz, R., Meeus, G., Montes, D., Olofsson, G., Su, K. Y. L., White, G. J., Barrado, D., Fukagawa, M., Grün, E., Kamp, I., Lorente, R., Morbidelli, A., Müller, S., Mutschke, H., Nakagawa, T., Ribas, I., and Walker, H. 2013. DUst around NEarby Stars. The survey observational results. *A&A*, **555**, A11.
- Esposito, L. W., Albers, N., Meinke, B. K., Sremčević, M., Madhusudhanan, P., Colwell, J. E., and Jorousek, R. G. 2012. A predator-prey model for moon-triggered clumping in Saturn's rings. *Icarus*, **217**, 103–114.
- Estrada, P. R., and Cuzzi, J. N. 1996. Voyager Observations of the Color of Saturn's Rings. *Icarus*, **122**, 251–272.
- Evans, II, N. J., Dunham, M. M., Jørgensen, J. K., Enoch, M. L., Merín, B., van Dishoeck, E. F., Alcalá, J. M., Myers, P. C., Stapelfeldt, K. R., Huard, T. L., Allen, L. E., Harvey, P. M., van Kempen, T., Blake, G. A., Koerner, D. W., Mundy, L. G., Padgett, D. L., and Sargent, A. I. 2009. The Spitzer c2d Legacy Results: Star-Formation Rates and Efficiencies; Evolution and Lifetimes. *ApJS*, **181**, 321–350.
- Fabian, A. C. 2012. Observational Evidence of Active Galactic Nuclei Feedback. *ARAA*, **50**, 455–489.
- Fan, X., Carilli, C. L., and Keating, B. 2006. Observational Constraints on Cosmic Reionization. *ARAA*, **44**, 415–462.
- Fanaroff, B. L., and Riley, J. M. 1974. The morphology of extragalactic radio sources of high and low luminosity. *MNRAS*, **167**, 31P–36P.
- Farihi, J., Jura, M., and Zuckerman, B. 2009. Infrared Signatures of Disrupted Minor Planets at White Dwarfs. *ApJ*, **694**, 805–819.
- Farinella, P., and Davis, D. R. 1996. Short-Period Comets: Primordial Bodies or Collisional Fragments? *Science*, **273**, 938–941.
- Faulkner, J., Lin, D. N. C., and Papaloizou, J. 1983. On the evolution of accretion disc flow in cataclysmic variables. I - The prospect of a limit cycle in dwarf nova systems. *MNRAS*, **205**, 359–375.
- Ferrarese, L., and Ford, H. 2005. Supermassive Black Holes in Galactic Nuclei: Past, Present and Future Research. *SSRv*, **116**, 523–624.
- Field, G. B. 1965. Thermal Instability. *ApJ*, **142**, 531.
- French, R. G., and Nicholson, P. D. 2000. Saturn's Rings II. Particle Sizes Inferred from Stellar Occultation Data. *Icarus*, **145**, 502–523.
- Fuller, J. 2014. Saturn ring seismology: Evidence for stable stratification in the deep interior of Saturn. *Icarus*, **242**, 283–296.
- Gałań, C., Mikołajewski, M., Tomov, T., Graczyk, D., Apostolovska, G., Barzova, I., Bellas-Velidis, I., Bilkina, B., Blake, R. M., Bolton, C. T., Bondar, A., Brát, L., Brożek, T., Budzisz, B., Cikała, M., Csák, B., Dapergolas, A., Dimitrov, D., Dobierski, P., Drahus, M., Drózdź, M., Dvorak, S., Elder, L., Frąckowiak, S., Galazutdinov, G., Gazeas, K., Georgiev, L., Gere, B., Goździewski, K., Grinin, V. P., Gromadzki, M., Hajduk, M., Heras, T. A., Hopkins, J., Iliev, I., Janowski, J., Kocián, R., Kołaczkowski, Z., Kolev, D., Kopacki, G., Krzesiński, J., Kučáková, H., Kuligowska, E., Kundera, T., Kurpińska-Winiarska, M., Kuźmicz, A., Liakos, A., Lister, T. A., Maciejewski, G., Majcher, A., Majewska, A., Marrese, P. M., Michalska, G., Migaszewski, C., Miller, I., Munari,

- U., Musaev, F., Myers, G., Narwid, A., Németh, P., Niarchos, P., Niemczura, E., Ogłóża, W., Ögmen, Y., Oksanen, A., Osiewala, J., Peneva, S., Pigulski, A., Popov, V., Pych, W., Pye, J., Ragan, E., Roukema, B. F., Rózański, P. T., Semkov, E., Siwak, M., Staels, B., Stateva, I., Stempels, H. C., Steśllicki, M., Świerczyński, E., Szymański, T., Tomov, N., Waniak, W., Więcek, M., Winiarski, M., Wychudzi, P., Zajczyk, A., Zola, S., and Zwitter, T. 2012. International observational campaigns of the last two eclipses in EE Cephei: 2003 and 2008/9. *A&A*, **544**(Aug.), A53.
- Gallagher, J. S., and Starrfield, S. 1978. Theory and observations of classical novae. *ARAA*, **16**, 171–214.
- Gammie, C. F. 1996. Layered Accretion in T Tauri Disks. *ApJ*, **457**, 355.
- Gammie, C. F. 2001. Nonlinear Outcome of Gravitational Instability in Cooling, Gaseous Disks. *ApJ*, **553**, 174–183.
- Gänsicke, B. T., Marsh, T. R., Southworth, J., and Rebassamansergas, A. 2006. A Gaseous Metal Disk Around a White Dwarf. *Science*, **314**, 1908–.
- Gänsicke, B. T., Koester, D., Farihi, J., Girven, J., Parsons, S. G., and Breedt, E. 2012. The chemical diversity of exo-terrestrial planetary debris around white dwarfs. *MNRAS*, **424**, 333–347.
- Garaud, P., Meru, F., Galvagni, M., and Olczak, C. 2013. From Dust to Planetesimals: An Improved Model for Collisional Growth in Protoplanetary Disks. *ApJ*, **764**, 146.
- Geretshauser, R. J., Speith, R., Güttler, C., Krause, M., and Blum, J. 2010. Numerical simulations of highly porous dust aggregates in the low-velocity collision regime. Implementation and calibration of a smooth particle hydrodynamics code. *A&A*, **513**, A58.
- Giacconi, R., Gursky, H., Paolini, F. R., and Rossi, B. B. 1962. Evidence for x Rays From Sources Outside the Solar System. *Physical Review Letters*, **9**, 439–443.
- Gierliński, M., and Done, C. 2004. Black hole accretion discs: reality confronts theory. *MNRAS*, **347**(Jan.), 885–894.
- Goertz, C. K., and Morfill, G. 1988. A new instability of Saturn's ring. *Icarus*, **74**, 325–330.
- Goldreich, P., and Lynden-Bell, D. 1965. II. Spiral arms as sheared gravitational instabilities. *MNRAS*, **130**, 125.
- Goldreich, P., and Porco, C. C. 1987a. Shepherding of the Uranian Rings. II. Dynamics. *AJ*, **93**, 730.
- Goldreich, P., and Porco, C. C. 1987b. Shepherding of the Uranian Rings. II. Dynamics. *AJ*, **93**(Mar.), 730.
- Goldreich, P., and Tremaine, S. 1978a. The excitation and evolution of density waves. *ApJ*, **222**, 850–858.
- Goldreich, P., and Tremaine, S. 1980. Disk-satellite interactions. *ApJ*, **241**(Oct.), 425–441.
- Goldreich, P., and Tremaine, S. 1981. The origin of the eccentricities of the rings of Uranus. *ApJ*, **243**(Feb.), 1062–1075.
- Goldreich, P., and Tremaine, S. 1982. The dynamics of planetary rings. *ARAA*, **20**, 249–283.
- Goldreich, P., and Tremaine, S. D. 1978b. The velocity dispersion in Saturn's rings. *Icarus*, **34**, 227–239.
- Gor'kavyj, N. N., and Fridman, A. M. 1994. *Physics of planetary rings. Celestial mechanics of continuous medium.*
- Graham, J. R., Matthews, K., Neugebauer, G., and Soifer, B. T. 1990. The infrared excess of G29-38 - A brown dwarf or dust? *ApJ*, **357**, 216–223.
- Greenberg, R., Hartmann, W. K., Chapman, C. R., and Wacker, J. F. 1978. Planetesimals to planets - Numerical simulation of collisional evolution. *Icarus*, **35**, 1–26.
- Greenstein, J. L., and Schmidt, M. 1964. The Quasi-Stellar Radio Sources 3c 48 and 3c 273. *ApJ*, **140**, 1.
- Guimarães, A. H. F., Albers, N., Spahn, F., Seiß, M., Vieira-Neto, E., and Brilliantov, N. V. 2012. Aggregates in the strength and gravity regime: Particles sizes in Saturn's rings. *Icarus*, **220**, 660–678.
- Gursky, H., Giacconi, R., Gorenstein, P., Waters, J. R., Oda, M., Bradt, H., Garmire, G., and Sreekantan, B. V. 1966. A Measurement of the Location of the X-Ray Source SCO X-1. *ApJ*, **146**, 310–316.
- Harris, A. W. 1984. The origin and evolution of planetary rings. Pages 641–659 of: Greenberg, R., and Brahic, A. (eds), *IAU Colloq. 75: Planetary Rings.*
- Hartman, R. C., Bertsch, D. L., Bloom, S. D., Chen, A. W., Deines-Jones, P., Esposito, J. A., Fichtel, C. E., Friedlander, D. P., Hunter, S. D., McDonald, L. M., Sreekumar, P., Thompson, D. J., Jones, B. B., Lin, Y. C., Michelson, P. F., Nolan, P. L., Tompkins, W. F., Kanbach, G., Mayer-Hasselwander, H. A., Mücke, A., Pohl, M., Reimer, O., Kniffen, D. A., Schneid, E. J., von Montigny, C., Mukherjee, R., and Dingus, B. L. 1999. The Third EGRET Catalog of High-Energy Gamma-Ray Sources. *ApJS*, **123**, 79–202.
- Hartmann, L., and Kenyon, S. J. 1996. The FU Orionis Phenomenon. *ARAA*, **34**, 207–240.
- Hatzes, A. P., Bridges, F. G., and Lin, D. N. C. 1988. Collisional properties of ice spheres at low impact velocities. *MNRAS*, **231**, 1091–1115.
- Hatzes, A. P., Bridges, F., Lin, D. N. C., and Sachtjen, S. 1991. Coagulation of particles in Saturn's rings - Measurements of the cohesive force of water frost. *Icarus*, **89**, 113–121.
- Hawley, J. F., Gammie, C. F., and Balbus, S. A. 1995. Local Three-dimensional Magnetohydrodynamic Simulations of Accretion Disks. *ApJ*, **440**, 742.
- Hedman, M. M., and Nicholson, P. D. 2013. Kronoseismology: Using Density Waves in Saturn's C Ring to Probe the Planet's Interior. *AJ*, **146**, 12.
- Hedman, M. M., Burns, J. A., Showalter, M. R., Porco, C. C., Nicholson, P. D., Bosh, A. S., Tiscareno, M. S., Brown, R. H., Buratti, B. J., Baines, K. H., and Clark, R. 2007. Saturn's dynamic D ring. *Icarus*, **188**, 89–107.
- Hedman, M. M., Murray, C. D., Cooper, N. J., Tiscareno, M. S., Beurle, K., Evans, M. W., and Burns, J. A. 2009. Three tenuous rings/arcs for three tiny moons. *Icarus*, **199**, 378–386.
- Hedman, M. M., Cooper, N. J., Murray, C. D., Beurle, K., Evans, M. W., Tiscareno, M. S., and Burns, J. A. 2010. Aegaeon (Saturn LIII), a G-ring object. *Icarus*, **207**, 433–447.
- Hedman, M. M., Burns, J. A., Evans, M. W., Tiscareno, M. S., and Porco, C. C. 2011. Saturn's Curiously Corrugated C Ring. *Science*, **332**, 708.
- Hedman, M. M., Nicholson, P. D., and Salo, H. 2014. Exploring Overstabilities in Saturn's A Ring Using Two Stellar Occultations. *AJ*, **148**, 15.
- Hellier, C. 2001. *Cataclysmic Variable Stars.*
- Herbig, G. H. 1977. Eruptive phenomena in early stellar evolution. *ApJ*, **217**(Nov.), 693–715.
- Herbig, G. H. 1989 (Sept.). FU Orionis eruptions. Pages 233–246 of: Reipurth, B. (ed), *European Southern Observatory Conference and Workshop Proceedings.* European Southern Observatory Conference and Workshop Proceedings, vol. 33.
- Hills, J. G. 1975. Possible power source of Seyfert galaxies and QSOs. *Nature*, **254**, 295–298.
- Hirose, S., Blaes, O., and Krolik, J. H. 2009. Turbulent Stresses in Local Simulations of Radiation-dominated Accretion Disks, and the Possibility of the Lightman-Eardley Instability. *ApJ*, **704**, 781–788.

- Hoard, D. W., Howell, S. B., and Stencel, R. E. 2010. Taming the Invisible Monster: System Parameter Constraints for epsilon Aurigae from the Far-ultraviolet to the Mid-infrared. *ApJ*, **714**(May), 549–560.
- Holberg, J. B., Barstow, M. A., and Green, E. M. 1997. The Discovery of Mg II  $\lambda$ 4481 in the White Dwarf EG 102: Evidence for Ongoing Accretion. *ApJL*, **474**, L127–L130.
- Horányi, M., Hartquist, T. W., Havnes, O., Mendis, D. A., and Morfill, G. E. 2004. Dusty plasma effects in Saturn’s magnetosphere. *Reviews of Geophysics*, **42**, 4002.
- Horányi, M., Burns, J. A., Hedman, M. M., Jones, G. H., and Kempf, S. 2009. *Diffuse Rings*. Page 511.
- Hubble, E. P. 1925. Cepheids in Spiral Nebulae. *Popular Astronomy*, **33**, 252–255.
- Hubble, E. P. 1936. *Realm of the Nebulae*.
- Hyodo, R., and Ohtsuki, K. 2014. Collisional Disruption of Gravitational Aggregates in the Tidal Environment. *ApJ*, **787**, 56.
- Hyodo, Ryuki, and Ohtsuki, Keiji. 2015. Saturn’s F ring and shepherd satellites a natural outcome of satellite system formation. *Nature Geoscience*, **8**(9), 686–689.
- Jeans, J. H. 1917. Some problems of astronomy (XXIV. The evolution of rotating masses). *The Observatory*, **40**, 196–203.
- Jewitt, D. C., and Luu, J. X. 2000. Physical Nature of the Kuiper Belt. *Protostars and Planets IV*, 1201.
- Jiang, Y.-F., Stone, J. M., and Davis, S. W. 2013. On the Thermal Stability of Radiation-dominated Accretion Disks. *ApJ*, **778**, 65.
- Johansen, A., Youdin, A., and Klahr, H. 2009. Zonal Flows and Long-lived Axisymmetric Pressure Bumps in Magnetorotational Turbulence. *ApJ*, **697**, 1269–1289.
- Johnson, B. M., and Gammie, C. F. 2003. Nonlinear Outcome of Gravitational Instability in Disks with Realistic Cooling. *ApJ*, **597**, 131–141.
- Joos, M., Hennebelle, P., and Ciardi, A. 2012. Protostellar disk formation and transport of angular momentum during magnetized core collapse. *A&A*, **543**, A128.
- Jura, M. 2003. A Tidally Disrupted Asteroid around the White Dwarf G29-38. *ApJL*, **584**, L91–L94.
- Jura, M. 2008. Pollution of Single White Dwarfs by Accretion of Many Small Asteroids. *AJ*, **135**, 1785–1792.
- Karjalainen, R. 2007. Aggregate impacts in Saturn’s rings. *Icarus*, **189**, 523–537.
- Karjalainen, R., and Salo, H. 2004. Gravitational accretion of particles in Saturn’s rings. *Icarus*, **172**, 328–348.
- Kato, S. 1978. Pulsational instability of accretion disks to axially symmetric oscillations. *MNRAS*, **185**, 629–642.
- Kato, S., and Yoshizawa, A. 1993. A model of hydromagnetic turbulence in accretion disks. *PASJ*, **45**, 103–112.
- Kato, S., and Yoshizawa, A. 1995. A Model of Hydromagnetic Turbulence in Accretion Disks. II. *PASJ*, **47**, 629–637.
- Katz, J. I. 1973. Thirty-five-day Periodicity in Her X-1. *Nature Physical Science*, **246**, 87–89.
- Kenyon, S. J., and Bromley, B. C. 2004a. Collisional Cascades in Planetesimal Disks. II. Embedded Planets. *AJ*, **127**, 513–530.
- Kenyon, S. J., and Bromley, B. C. 2004b. Detecting the Dusty Debris of Terrestrial Planet Formation. *ApJL*, **602**, L133–L136.
- Kenyon, S. J., and Hartmann, L. 1995. Pre-Main-Sequence Evolution in the Taurus-Auriga Molecular Cloud. *ApJS*, **101**, 117.
- Kesden, M. 2012. Tidal-disruption rate of stars by spinning supermassive black holes. *PhRvD*, **85**(2), 024037.
- King, A. R. 2006. *Accretion in compact binaries*. Pages 507–546.
- Klein, B., Jura, M., Koester, D., Zuckerman, B., and Melis, C. 2010. Chemical Abundances in the Externally Polluted White Dwarf GD 40: Evidence of a Rocky Extrasolar Minor Planet. *ApJ*, **709**, 950–962.
- Kley, W., Papaloizou, J. C. B., and Lin, D. N. C. 1993. Two-dimensional viscous accretion disk models. II - On viscous overstability. *ApJ*, **409**, 739–747.
- Kobayashi, S., Laguna, P., Phinney, E. S., and Mészáros, P. 2004. Gravitational Waves and X-Ray Signals from Stellar Disruption by a Massive Black Hole. *ApJ*, **615**, 855–865.
- Koerner, D. W., Sargent, A. I., and Beckwith, S. V. W. 1993. A rotating gaseous disk around the T Tauri star GM Aurigae. *Icarus*, **106**(Nov.), 2.
- Koester, D., Provencal, J., and Shipman, H. L. 1997. Metals in the variable DA G29-38. *A&A*, **320**, L57–L59.
- Kokubo, E., and Ida, S. 1996. On Runaway Growth of Planetesimals. *Icarus*, **123**, 180–191.
- Kokubo, E., and Ida, S. 1998. Oligarchic Growth of Protoplanets. *Icarus*, **131**, 171–178.
- Komossa, S., and Bade, N. 1999. The giant X-ray outbursts in NGC 5905 and IC 3599:() hfill Follow-up observations and outburst scenarios. *A&A*, **343**, 775–787.
- Kormendy, J., and Richstone, D. 1995. Inward Bound—The Search For Supermassive Black Holes In Galactic Nuclei. *ARAA*, **33**, 581.
- Korycansky, D. G., and Pringle, J. E. 1995. Axisymmetric waves in polytropic accretion discs. *MNRAS*, **272**, 618–624.
- Kotze, M. M., and Charles, P. A. 2012. Characterizing X-ray binary long-term variability. *MNRAS*, **420**, 1575–1589.
- Kraft, R. P. 1962. Binary Stars among Cataclysmic Variables. I. U Geminorum Stars (dwarf Novae). *ApJ*, **135**, 408.
- Kraft, R. P. 1964. Binary Stars among Cataclysmic Variables. III. Ten Old Novae. *ApJ*, **139**, 457.
- Kral, Q., Thébault, P., and Charnoz, S. 2013. LIDT-DD: A new self-consistent debris disc model that includes radiation pressure and couples dynamical and collisional evolution. *A&A*, **558**, A121.
- Krivov, A. V., Löhne, T., and Sremčević, M. 2006. Dust distributions in debris disks: effects of gravity, radiation pressure and collisions. *A&A*, **455**, 509–519.
- Kuiper, G. P. 1951. On the Origin of the Solar System. *Proceedings of the National Academy of Science*, **37**, 1–14.
- Kunz, M. W., Schekochihin, A. A., and Stone, J. M. 2014. Firehose and Mirror Instabilities in a Collisionless Shearing Plasma. *Physical Review Letters*, **112**(20), 205003.
- Lada, C. J., and Wilking, B. A. 1984. The nature of the embedded population in the Rho Ophiuchi dark cloud - Mid-infrared observations. *ApJ*, **287**, 610–621.
- Lagrange, A.-M., Gratadour, D., Chauvin, G., Fusco, T., Ehrenreich, D., Mouillet, D., Rousset, G., Rouan, D., Allard, F., Gendron, É., Charton, J., Mugnier, L., Rabou, P., Montri, J., and Lacombe, F. 2009. A probable giant planet imaged in the  $\beta$  Pictoris disk. VLT/NaCo deep L’-band imaging. *A&A*, **493**, L21–L25.
- Lambrechts, M., and Johansen, A. 2012. Rapid growth of gaseous cores by pebble accretion. *A&A*, **544**, A32.
- Lasota, J.-P. 2001. The disc instability model of dwarf novae and low-mass X-ray binary transients. *NewAR*, **45**, 449–508.
- Latter, H. N., and Ogilvie, G. I. 2006a. The linear stability of dilute particulate rings. *Icarus*, **184**, 498–516.

- Latter, H. N., and Ogilvie, G. I. 2006b. Viscous overstability and eccentricity evolution in three-dimensional gaseous discs. *MNRAS*, **372**, 1829–1839.
- Latter, H. N., and Ogilvie, G. I. 2008. Dense planetary rings and the viscous overstability. *Icarus*, **195**, 725–751.
- Latter, H. N., and Ogilvie, G. I. 2009. The viscous overstability, nonlinear wavetrains, and finescale structure in dense planetary rings. *Icarus*, **202**(Aug.), 565–583.
- Latter, H. N., and Ogilvie, G. I. 2010. Hydrodynamical simulations of viscous overstability in Saturn’s rings. *Icarus*, **210**, 318–329.
- Latter, H. N., and Papaloizou, J. C. B. 2012. Hysteresis and thermal limit cycles in MRI simulations of accretion discs. *MNRAS*, **426**, 1107–1120.
- Latter, H. N., Ogilvie, G. I., and Chupeau, M. 2012a. The ballistic transport instability in Saturn’s rings - I. Formalism and linear theory. *MNRAS*, **427**, 2336–2348.
- Latter, H. N., Rein, H., and Ogilvie, G. I. 2012b. The gravitational instability of a stream of co-orbital particles. *MNRAS*, **423**(June), 1267–1276.
- Latter, H. N., Ogilvie, G. I., and Chupeau, M. 2014a. The ballistic transport instability in Saturn’s rings - II. Non-linear wave dynamics. *MNRAS*, **441**, 2760–2772.
- Latter, H. N., Ogilvie, G. I., and Chupeau, M. 2014b. The ballistic transport instability in Saturn’s rings - III. Numerical simulations. *MNRAS*, **441**, 2773–2781.
- Leinhardt, Z. M., and Richardson, D. C. 2002. N-Body Simulations of Planetesimal Evolution: Effect of Varying Impactor Mass Ratio. *Icarus*, **159**, 306–313.
- Leinhardt, Z. M., and Stewart, S. T. 2012. Collisions between Gravity-dominated Bodies. I. Outcome Regimes and Scaling Laws. *ApJ*, **745**, 79.
- Leinhardt, Z. M., Ogilvie, G. I., Latter, H. N., and Kokubo, E. 2012. Tidal disruption of satellites and formation of narrow rings. *MNRAS*, **424**, 1419–1431.
- Lesur, G., and Ogilvie, G. I. 2010. On the angular momentum transport due to vertical convection in accretion discs. *MNRAS*, **404**, L64–L68.
- Lesur, G., and Papaloizou, J. C. B. 2010a. The subcritical baroclinic instability in local accretion disc models. *A&A*, **513**, A60.
- Lesur, G., and Papaloizou, J. C. B. 2010b. The subcritical baroclinic instability in local accretion disc models. *A&A*, **513**, A60.
- Lesur, G., Hennebelle, P., and Fromang, S. 2015. Spiral-driven accretion in protoplanetary discs. I. 2D models. *A&A*, **582**, L9.
- Lewis, M. C., and Stewart, G. R. 2000. Collisional Dynamics of Perturbed Planetary Rings. I. *AJ*, **120**, 3295–3310.
- Lewis, M. C., and Stewart, G. R. 2009. Features around embedded moonlets in Saturn’s rings: The role of self-gravity and particle size distributions. *Icarus*, **199**, 387–412.
- Lightman, A. P., and Eardley, D. M. 1974. Black Holes in Binary Systems: Instability of Disk Accretion. *ApJL*, **187**, L1.
- Lin, C. C., and Shu, F. H. 1964. On the Spiral Structure of Disk Galaxies. *ApJ*, **140**, 646.
- Lin, D. N. C., and Bodenheimer, P. 1981. On the stability of Saturn’s rings. *ApJL*, **248**, L83–L86.
- Lin, D. N. C., and Papaloizou, J. 1986. On the tidal interaction between protoplanets and the protoplanetary disk. III - Orbital migration of protoplanets. *ApJ*, **309**(Oct.), 846–857.
- Lin, D. N. C., and Papaloizou, J. C. B. 1993. On the tidal interaction between protostellar disks and companions. Pages 749–835 of: Levy, E. H., and Lunine, J. I. (eds), *Protostars and Planets III*.
- Lissauer, J. J., Squyres, S. W., and Hartmann, W. K. 1988. Bombardment history of the Saturn system. *JGR*, **93**, 13776–13804.
- Löhne, T., Augereau, J.-C., Ertel, S., Marshall, J. P., Eiroa, C., Mora, A., Absil, O., Stapelfeldt, K., Thébault, P., Bayo, A., Del Burgo, C., Danchi, W., Krivov, A. V., Lebreton, J., Letawe, G., Magain, P., Maldonado, J., Montesinos, B., Pilbratt, G. L., White, G. J., and Wolf, S. 2012. Modelling the huge, Herschel-resolved debris ring around HD 207129. *A&A*, **537**, A110.
- Longaretti, P.-Y. 1989. Saturn’s main ring particle size distribution - an analytic approach. *Icarus*, **81**, 51–73.
- Longaretti, P.-Y., and Rappaport, N. 1995. Viscous overstabilities in dense narrow planetary rings. *Icarus*, **116**, 376–396.
- Loska, Z. 1986. Three-dimensional waves in disks. *AcA*, **36**, 43–61.
- Lubow, S. H. 1991. A model for tidally driven eccentric instabilities in fluid disks. *ApJ*, **381**(Nov.), 259–267.
- Lubow, S. H., and Ogilvie, G. I. 2001. Secular Interactions between Inclined Planets and a Gaseous Disk. *ApJ*, **560**(Oct.), 997–1009.
- Lubow, S. H., and Pringle, J. E. 1993. Wave propagation in accretion disks - Axisymmetric case. *ApJ*, **409**, 360–371.
- Lukkari, J. 1981. Collisional amplification of density fluctuations in Saturn’s rings. *Nature*, **292**, 433–435.
- Lynden-Bell, D. 1967. Statistical mechanics of violent relaxation in stellar systems. *MNRAS*, **136**, 101.
- Lynden-Bell, D. 1969. Galactic Nuclei as Collapsed Old Quasars. *Nature*, **223**(Aug.), 690–694.
- Lynden-Bell, D., and Pringle, J. E. 1974. The evolution of viscous discs and the origin of the nebular variables. *MNRAS*, **168**, 603–637.
- Lyubarskij, Y. E., Postnov, K. A., and Prokhorov, M. E. 1994. Eccentric Accretion Discs. *MNRAS*, **266**, 583.
- Macchetto, F., Marconi, A., Axon, D. J., Capetti, A., Sparks, W., and Crane, P. 1997. The Supermassive Black Hole of M87 and the Kinematics of Its Associated Gaseous Disk. *ApJ*, **489**, 579–600.
- Marconi, A., Risaliti, G., Gilli, R., Hunt, L. K., Maiolino, R., and Salvati, M. 2004. Local supermassive black holes, relics of active galactic nuclei and the X-ray background. *MNRAS*, **351**, 169–185.
- Marino, S., Perez, S., and Casassus, S. 2015a. Shadows Cast by a Warp in the HD 142527 Protoplanetary Disk. *ApJL*, **798**(Jan.), L44.
- Marino, S., Perez, S., and Casassus, S. 2015b. Shadows Cast by a Warp in the HD 142527 Protoplanetary Disk. *ApJL*, **798**, L44.
- Marley, M. S. 1991. Nonradial oscillations of Saturn. *Icarus*, **94**, 420–435.
- Masset, F. S., Morbidelli, A., Crida, A., and Ferreira, J. 2006. Disk Surface Density Transitions as Protoplanet Traps. *ApJ*, **642**(May), 478–487.
- Matthews, B. C., Krivov, A. V., Wyatt, M. C., Bryden, G., and Eiroa, C. 2014. Observations, Modeling, and Theory of Debris Disks. *Protostars and Planets VI*, 521–544.
- Mayor, M., and Queloz, D. 1995. A Jupiter-mass companion to a solar-type star. *Nature*, **378**, 355–359.
- McCaughrean, M. J., and O’Dell, C. R. 1996. Direct Imaging of Circumstellar Disks in the Orion Nebula. *AJ*, **111**, 1977.
- McConnell, N. J., Ma, C.-P., Gebhardt, K., Wright, S. A., Murphy, J. D., Lauer, T. R., Graham, J. R., and Richstone, D. O.

2011. Two ten-billion-solar-mass black holes at the centres of giant elliptical galaxies. *Nature*, **480**, 215–218.
- McKee, C. F., and Ostriker, E. C. 2007. Theory of Star Formation. *ARAA*, **45**, 565–687.
- McKee, C. F., and Ostriker, J. P. 1977. A theory of the interstellar medium - Three components regulated by supernova explosions in an inhomogeneous substrate. *ApJ*, **218**, 148–169.
- Meinke, B. K., Esposito, L. W., Albers, N., and Sremčević, M. 2012. Classification of F ring features observed in Cassini UVIS occultations. *Icarus*, **218**, 545–554.
- Merritt, D. 2013. *Dynamics and Evolution of Galactic Nuclei*.
- Meyer, F., and Meyer-Hofmeister, E. 1981. On the Elusive Cause of Cataclysmic Variable Outbursts. *A&A*, **104**, L10.
- Miley, G., and De Breuck, C. 2008. Distant radio galaxies and their environments. *AARv*, **15**, 67–144.
- Miranda, R., Horák, J., and Lai, D. 2015. Viscous driving of global oscillations in accretion discs around black holes. *MNRAS*, **446**, 240–253.
- Miyoshi, M., Moran, J., Herrnstein, J., Greenhill, L., Nakai, N., Diamond, P., and Inoue, M. 1995. Evidence for a black hole from high rotation velocities in a sub-parsec region of NGC4258. *Nature*, **373**, 127–129.
- Montmerle, T., Augereau, J.-C., Chaussidon, M., Gounelle, M., Marty, B., and Morbidelli, A. 2006. From Suns to Life: A Chronological Approach to the History of Life on Earth 3. Solar System Formation and Early Evolution: the First 100 Million Years. *Earth Moon and Planets*, **98**, 39–95.
- Mouillet, D., Larwood, J. D., Papaloizou, J. C. B., and Lagrange, A. M. 1997. A planet on an inclined orbit as an explanation of the warp in the Beta Pictoris disc. *MNRAS*, **292**, 896.
- Murray, C. D., Chavez, C., Beurle, K., Cooper, N., Evans, M. W., Burns, J. A., and Porco, C. C. 2005. How Prometheus creates structure in Saturn’s F ring. *Nature*, **437**, 1326–1329.
- Muto, T., Grady, C. A., Hashimoto, J., Fukagawa, M., Hornbeck, J. B., Sitko, M., Russell, R., Werren, C., Curé, M., Currie, T., Ohashi, N., Okamoto, Y., Momose, M., Honda, M., Inutsuka, S., Takeuchi, T., Dong, R., Abe, L., Brandner, W., Brandt, T., Carson, J., Egner, S., Feldt, M., Fukue, T., Goto, M., Guyon, O., Hayano, Y., Hayashi, M., Hayashi, S., Henning, T., Hodapp, K. W., Ishii, M., Iye, M., Janson, M., Kandori, R., Knapp, G. R., Kudo, T., Kusakabe, N., Kuzuhara, M., Matsuo, T., Mayama, S., McElwain, M. W., Miyama, S., Morino, J.-I., Moro-Martin, A., Nishimura, T., Pyo, T.-S., Serabyn, E., Suto, H., Suzuki, R., Takami, M., Takato, N., Terada, H., Thalmann, C., Tomono, D., Turner, E. L., Watanabe, M., Wisniewski, J. P., Yamada, T., Takami, H., Usuda, T., and Tamura, M. 2012. Discovery of Small-scale Spiral Structures in the Disk of SAO 206462 (HD 135344B): Implications for the Physical State of the Disk from Spiral Density Wave Theory. *ApJL*, **748**, L22.
- Narayan, R., and Yi, I. 1994. Advection-dominated accretion: A self-similar solution. *ApJL*, **428**, L13–L16.
- Narayan, R., Mahadevan, R., and Quataert, E. 1998. Advection-dominated accretion around black holes. Pages 148–182 of: Abramowicz, M. A., Björnsson, G., and Pringle, J. E. (eds), *Theory of Black Hole Accretion Disks*.
- Nelson, R. P., and Papaloizou, J. C. B. 2004. The interaction of giant planets with a disc with MHD turbulence - IV. Migration rates of embedded protoplanets. *MNRAS*, **350**, 849–864.
- Nelson, R. P., Gressel, O., and Umurhan, O. M. 2013. Linear and non-linear evolution of the vertical shear instability in accretion discs. *MNRAS*, **435**, 2610–2632.
- Nesvold, E. R., Kuchner, M. J., Rein, H., and Pan, M. 2013. SMACK: A New Algorithm for Modeling Collisions and Dynamics of Planetesimals in Debris Disks. *ApJ*, **777**, 144.
- Netzer, H. 2015. Revisiting the Unified Model of Active Galactic Nuclei. *ARAA*, **53**, 365–408.
- Nicholson, P. D., French, R. G., Hedman, M. M., Marouf, E. A., and Colwell, J. E. 2014. Noncircular features in Saturn’s rings I: The edge of the B ring. *Icarus*, **227**, 152–175.
- Ogilvie, G. I. 1998. Waves and instabilities in a differentially rotating disc containing a poloidal magnetic field. *MNRAS*, **297**, 291–314.
- Ogilvie, G. I. 1999. The non-linear fluid dynamics of a warped accretion disc. *MNRAS*, **304**, 557–578.
- Ogilvie, G. I. 2001. Non-linear fluid dynamics of eccentric discs. *MNRAS*, **325**, 231–248.
- Ogilvie, G. I. 2003. On the dynamics of magnetorotational turbulent stresses. *MNRAS*, **340**, 969–982.
- Ogilvie, G. I. 2006. Non-linear bending waves in Keplerian accretion discs. *MNRAS*, **365**, 977–990.
- Ogilvie, G. I., and Lubow, S. H. 2002. On the wake generated by a planet in a disc. *MNRAS*, **330**(Mar.), 950–954.
- Okazaki, A. T. 1991. Long-term V/R variations of Be stars due to global one-armed oscillations of equatorial disks. *PASJ*, **43**, 75–94.
- Okazaki, A. T., Kato, S., and Fukue, J. 1987. Global trapped oscillations of relativistic accretion disks. *PASJ*, **39**, 457–473.
- Paardekooper, S.-J. 2012. Numerical convergence in self-gravitating shearing sheet simulations and the stochastic nature of disc fragmentation. *MNRAS*, **421**, 3286–3299.
- Paardekooper, S.-J., and Papaloizou, J. C. B. 2008. On disc protoplanet interactions in a non-barotropic disc with thermal diffusion. *A&A*, **485**(July), 877–895.
- Paardekooper, S.-J., and Papaloizou, J. C. B. 2009. On corotation torques, horseshoe drag and the possibility of sustained stalled or outward protoplanetary migration. *MNRAS*, **394**(Apr.), 2283–2296.
- Paczynski, B. 1977. A model of accretion disks in close binaries. *ApJ*, **216**(Sept.), 822–826.
- Papaloizou, J., and Pringle, J. E. 1977. Tidal torques on accretion discs in close binary systems. *MNRAS*, **181**(Nov.), 441–454.
- Papaloizou, J. C., and Savonije, G. J. 1991. Instabilities in self-gravitating gaseous discs. *MNRAS*, **248**(Feb.), 353–369.
- Papaloizou, J. C. B., and Lin, D. N. C. 1988. On the pulsational overinstability in narrowly confined viscous rings. *ApJ*, **331**, 838–860.
- Papaloizou, J. C. B., and Lin, D. N. C. 1995. On the dynamics of warped accretion disks. *ApJ*, **438**, 841–851.
- Papaloizou, J. C. B., and Stanley, G. Q. G. 1986. The structure and stability of the accretion disc boundary layer. *MNRAS*, **220**, 593–610.
- Papaloizou, J. C. B., and Terquem, C. 2006. Planet formation and migration. *Reports on Progress in Physics*, **69**, 119–180.
- Patterson, J., Kemp, J., Jensen, L., Vanmunster, T., Skillman, D. R., Martin, B., Fried, R., and Thorstensen, J. R. 2000. Superhumps in Cataclysmic Binaries. XVIII. IY Ursae Majoris. *PASP*, **112**(Dec.), 1567–1583.
- Peale, S. J. 1999. Origin and Evolution of the Natural Satellites. *ARAA*, **37**, 533–602.
- Pérez, L. M., Isella, A., Carpenter, J. M., and Chandler, C. J. 2014. Large-scale Asymmetries in the Transitional Disks of SAO 206462 and SR 21. *ApJL*, **783**, L13.

- Perrine, R. P., and Richardson, D. C. 2012. N-body simulations of cohesion in dense planetary rings: A study of cohesion parameters. *Icarus*, **219**, 515–533.
- Perrine, R. P., Richardson, D. C., and Scheeres, D. J. 2011. A numerical model of cohesion in planetary rings. *Icarus*, **212**, 719–735.
- Peterson, B. M. 2001. Variability of Active Galactic Nuclei. Page 3 of: Aretxaga, I., Kunth, D., and Mújica, R. (eds), *Advanced Lectures on the Starburst-AGN*.
- Petit, J.-M., Kavelaars, J. J., Gladman, B., and Loredó, T. 2008. *Size Distribution of Multikilometer Transneptunian Objects*. Pages 71–87.
- Piran, T. 1978. The role of viscosity and cooling mechanisms in the stability of accretion disks. *ApJ*, **221**, 652–660.
- Pollack, J. B. 1975. The rings of Saturn. *SSRv*, **18**, 3–93.
- Pollack, J. B., Grossman, A. S., Moore, R., and Graboske, Jr., H. C. 1976. The formation of Saturn’s satellites and rings, as influenced by Saturn’s contraction history. *Icarus*, **29**, 35–48.
- Pringle, J. E. 1981. Accretion discs in astrophysics. *ARAA*, **19**, 137–162.
- Pudritz, R. E., Ouyed, R., Fendt, C., and Brandenburg, A. 2007. Disk Winds, Jets, and Outflows: Theoretical and Computational Foundations. *Protostars and Planets V*, 277–294.
- Quataert, E., and Chiang, E. I. 2000. Angular Momentum Transport in Particle and Fluid Disks. *ApJ*, **543**, 432–437.
- Quillen, A. C. 2006. Predictions for a planet just inside Fomalhaut’s eccentric ring. *MNRAS*, **372**, L14–L18.
- Quirrenbach, A., Buscher, D. F., Mozurkewich, D., Hummel, C. A., and Armstrong, J. T. 1994. Maximum-entropy maps of the Be shell star zeta Tauri from optical long-baseline interferometry. *A&A*, **283**, L13–L16.
- Rees, M. J. 1984. Black Hole Models for Active Galactic Nuclei. *ARAA*, **22**, 471–506.
- Rees, M. J. 1988. Tidal disruption of stars by black holes of 10 to the 6th-10 to the 8th solar masses in nearby galaxies. *Nature*, **333**, 523–528.
- Rees, M. J., Begelman, M. C., Blandford, R. D., and Phinney, E. S. 1982. Ion-supported tori and the origin of radio jets. *Nature*, **295**, 17–21.
- Rein, H. 2012. Planet-disc interaction in highly inclined systems. *MNRAS*, **422**, 3611–3616.
- Rein, H., and Latter, H. N. 2013. Large-scale N-body simulations of the viscous overstability in Saturn’s rings. *MNRAS*, **431**, 145–158.
- Rein, H., and Papaloizou, J. C. B. 2009. On the evolution of mean motion resonances through stochastic forcing: fast and slow libration modes and the origin of HD 128311. *A&A*, **497**, 595–609.
- Rein, H., and Papaloizou, J. C. B. 2010. Stochastic orbital migration of small bodies in Saturn’s rings. *A&A*, **524**, A22+.
- Remillard, R. A., and McClintock, J. E. 2006. X-Ray Properties of Black-Hole Binaries. *ARAA*, **44**, 49–92.
- Rice, W. K. M., Lodato, G., and Armitage, P. J. 2005. Investigating fragmentation conditions in self-gravitating accretion discs. *MNRAS*, **364**, L56–L60.
- Rice, W. K. M., Paardekooper, S.-J., Forgan, D. H., and Armitage, P. J. 2014. Convergence of simulations of self-gravitating accretion discs - II. Sensitivity to the implementation of radiative cooling and artificial viscosity. *MNRAS*, **438**, 1593–1602.
- Richardson, D. C., Quinn, T., Stadel, J., and Lake, G. 2000. Direct Large-Scale N-Body Simulations of Planetesimal Dynamics. *Icarus*, **143**, 45–59.
- Ringl, C., Bringa, E. M., Bertoldi, D. S., and Urbassek, H. M. 2012. Collisions of Porous Clusters: A Granular-mechanics Study of Compaction and Fragmentation. *ApJ*, **752**, 151.
- Rivinius, T., Carciofi, A. C., and Martayan, C. 2013. Classical Be stars. Rapidly rotating B stars with viscous Keplerian decretion disks. *AARv*, **21**, 69.
- Safronov, V. S. 1969. Evolution of the Protoplanetary Cloud and Formation of the Earth and the Planets. *Nauka, Moscow (NASA technical Translation TTF-677)*.
- Salo, H. 1991. Numerical simulations of dense collisional systems. *Icarus*, **90**, 254–270.
- Salo, H. 1992. Gravitational wakes in Saturn’s rings. *Nature*, **359**, 619–621.
- Salo, H. 1995. Simulations of dense planetary rings. III. Self-gravitating identical particles. *Icarus*, **117**, 287–312.
- Salo, H., and Schmidt, J. 2010. N-body simulations of viscous instability of planetary rings. *Icarus*, **206**, 390–409.
- Salo, H., Schmidt, J., and Spahn, F. 2001. Viscous Overstability in Saturn’s B Ring. I. Direct Simulations and Measurement of Transport Coefficients. *Icarus*, **153**, 295–315.
- Salpeter, E. E. 1964. Accretion of Interstellar Matter by Massive Objects. *ApJ*, **140**(Aug.), 796–800.
- Sanchis-Ojeda, R., Rappaport, S., Pallè, E., Delrez, L., DeVore, J., Gandolfi, D., Fukui, A., Ribas, I., Stassun, K. G., Albrecht, S., Dai, F., Gaidos, E., Gillon, M., Hirano, T., Holman, M., Howard, A. W., Isaacson, H., Jehin, E., Kuzuhara, M., Mann, A. W., Marcy, G. W., Miles-Páez, P. A., Montañés-Rodríguez, P., Murgas, F., Narita, N., Nowak, G., Onitsuka, M., Paegert, M., Van Eylen, V., Winn, J. N., and Yu, L. 2015. The K2-ESPRINT Project I: Discovery of the Disintegrating Rocky Planet K2-22b with a Cometary Head and Leading Tail. *ApJ*, **812**, 112.
- Sandage, A., Osmer, P., Giacconi, R., Gorenstein, P., Gursky, H., Waters, J., Bradt, H., Garmire, G., Sreekantan, B. V., Oda, M., Osawa, K., and Jugaku, J. 1966. On the optical identification of SCO X-1. *ApJ*, **146**, 316.
- Sargent, A. I., and Beckwith, S. 1987. Kinematics of the circumstellar gas of HL Tauri and R Monocerotis. *ApJ*, **323**(Dec.), 294–305.
- Savage, S. B., and Jeffrey, D. J. 1981. The stress tensor in a granular flow at high shear rates. *Journal of Fluid Mechanics*, **110**, 255–272.
- Schmidt, J., and Salo, H. 2003. Weakly Nonlinear Model for Oscillatory Instability in Saturn’s Dense Rings. *Physical Review Letters*, **90**(6), 061102.
- Schmidt, J., Salo, H., Spahn, F., and Petzschmann, O. 2001. Viscous Overstability in Saturn’s B-Ring. II. Hydrodynamic Theory and Comparison to Simulations. *Icarus*, **153**, 316–331.
- Schmit, U., and Tscharnuter, W. M. 1995. A fluid dynamical treatment of the common action of self-gravitation, collisions, and rotation in Saturn’s B-ring. *Icarus*, **115**, 304–319.
- Schmit, U., and Tscharnuter, W. M. 1999. On the Formation of the Fine-Scale Structure in Saturn’s B Ring. *Icarus*, **138**, 173–187.
- Searle, L., and Zinn, R. 1978. Compositions of halo clusters and the formation of the galactic halo. *ApJ*, **225**, 357–379.
- Seizinger, A., and Kley, W. 2013. Bouncing behavior of microscopic dust aggregates. *A&A*, **551**, A65.
- Sfair, R., Winter, S. M. G., Mourão, D. C., and Winter, O. C. 2009. Dynamical evolution of Saturn’s F ring dust particles. *MNRAS*, **395**, 2157–2161.
- Shakura, N. I., and Sunyaev, R. A. 1973. Black holes in binary systems. Observational appearance. *A&A*, **24**, 337–355.

- Shakura, N. I., and Sunyaev, R. A. 1976. A theory of the instability of disk accretion on to black holes and the variability of binary X-ray sources, galactic nuclei and quasars. *MNRAS*, **175**, 613–632.
- Shara, M. M. 1989. Recent progress in understanding the eruptions of classical novae. *PASP*, **101**, 5–31.
- Showalter, M. R., Hedman, M. M., and Burns, J. A. 2011. The Impact of Comet Shoemaker-Levy 9 Sends Ripples Through the Rings of Jupiter. *Science*, **332**, 711.
- Shu, F. H. 1992. *The physics of astrophysics. Volume II: Gas dynamics*.
- Shu, F. H., and Stewart, G. R. 1985. The collisional dynamics of particulate disks. *Icarus*, **62**, 360–383.
- Smak, J. 1971. Eruptive Binaries. II. U Geminorum. *AcA*, **21**, 15.
- Smith, B. A., Soderblom, L. A., Banfield, D., Barnet, C., Basilevsky, A. T., Beebe, R. F., Bollinger, K., Boyce, J. M., Brahic, A., Briggs, G. A., Brown, R. H., Chyba, C., Collins, S. A., Colvin, T., Cook, A. F., Crisp, D., Croft, S. K., Cruikshank, D., Cuzzi, J. N., Danielson, G. E., Davies, M. E., de Jong, E., Dones, L., Godfrey, D., Goguen, J., Grenier, I., Haemmerle, V. R., Hammel, H., Hansen, C. J., Helfenstein, C. P., Howell, C., Hunt, G. E., Ingersoll, A. P., Johnson, T. V., Kargel, J., Kirk, R., Kuehn, D. I., Limaye, S., Matarsky, H., McEwen, A., Morrison, D., Owen, T., Owen, W., Pollack, J. B., Porco, C. C., Rages, K., Rogers, P., Rudy, D., Sagan, C., Schwartz, J., Shoemaker, E. M., Showalter, M., Siscardy, B., Simonelli, D., Spencer, J., Stromovsky, L. A., Stoker, C., Strom, R. G., Suomi, V. E., Synott, S. P., Terrile, R. J., Thomas, P., Thompson, W. R., Verbiscer, A., and Veverka, J. 1989. Voyager 2 at Neptune: Imaging Science Results. *Science*, **246**, 1422–1449.
- Spahn, F., Hertzsch, J.-M., and Brilliantov, N. V. 1995. The role of particle collisions for the dynamics in planetary rings. *Chaos Solitons and Fractals*, **5**, 1945–1964.
- Spitale, J. N., and Porco, C. C. 2010. Detection of Free Unstable Modes and Massive Bodies in Saturn’s Outer B Ring. *AJ*, **140**, 1747–1757.
- Springel, V., White, S. D. M., Jenkins, A., Frenk, C. S., Yoshida, N., Gao, L., Navarro, J., Thacker, R., Croton, D., Helly, J., Peacock, J. A., Cole, S., Thomas, P., Couchman, H., Evrard, A., Colberg, J., and Pearce, F. 2005. Simulations of the formation, evolution and clustering of galaxies and quasars. *Nature*, **435**, 629–636.
- Stansberry, J., Grundy, W., Brown, M., Cruikshank, D., Spencer, J., Trilling, D., and Margot, J.-L. 2008. *Physical Properties of Kuiper Belt and Centaur Objects: Constraints from the Spitzer Space Telescope*. Pages 161–179.
- Strubbe, L. E., and Quataert, E. 2009. Optical flares from the tidal disruption of stars by massive black holes. *MNRAS*, **400**, 2070–2084.
- Su, K. Y. L., Rieke, G. H., Stansberry, J. A., Bryden, G., Stapelfeldt, K. R., Trilling, D. E., Muzerolle, J., Beichman, C. A., Moro-Martin, A., Hines, D. C., and Werner, M. W. 2006. Debris Disk Evolution around A Stars. *ApJ*, **653**, 675–689.
- Su, K. Y. L., Rieke, G. H., Stapelfeldt, K. R., Malhotra, R., Bryden, G., Smith, P. S., Misselt, K. A., Moro-Martin, A., and Williams, J. P. 2009. The Debris Disk Around HR 8799. *ApJ*, **705**(Nov.), 314–327.
- Supulver, K. D., Bridges, F. G., and Lin, D. N. C. 1995. The coefficient of restitution of ice particles in glancing collisions: Experimental results for unfrosted surfaces. *Icarus*, **113**, 188–199.
- Supulver, K. D., Bridges, F. G., Tiscareno, S., Lievore, J., and Lin, D. N. C. 1997. The Sticking Properties of Water Frost Produced under Various Ambient Conditions. *Icarus*, **129**, 539–554.
- Takahashi, S. Z., and Inutsuka, S.-i. 2014. Two-component Secular Gravitational Instability in a Protoplanetary Disk: A Possible Mechanism for Creating Ring-like Structures. *ApJ*, **794**, 55.
- Tamayo, D., Triaud, A. H. M. J., Menou, K., and Rein, H. 2015. Dynamical Stability of Imaged Planetary Systems in Formation: Application to HL Tau. *ApJ*, **805**, 100.
- Tanaka, H., Inaba, S., and Nakazawa, K. 1996. Steady-State Size Distribution for the Self-Similar Collision Cascade. *Icarus*, **123**(Oct.), 450–455.
- Tauris, T. M., and van den Heuvel, E. P. J. 2006. *Formation and evolution of compact stellar X-ray sources*. Pages 623–665.
- Testi, L., Birnstiel, T., Ricci, L., Andrews, S., Blum, J., Carpenter, J., Dominik, C., Isella, A., Natta, A., Williams, J. P., and Wilner, D. J. 2014. Dust Evolution in Protoplanetary Disks. *Protostars and Planets VI*, 339–361.
- Teyssandier, J., and Ogilvie, G. I. 2016. Growth of eccentric modes in disc-planet interactions. *MNRAS*, **458**(May), 3221–3247.
- Thébault, P., and Augereau, J.-C. 2007. Collisional processes and size distribution in spatially extended debris discs. *A&A*, **472**, 169–185.
- Thompson, W. T., Lumme, K., Irvine, W. M., Baum, W. A., and Esposito, L. W. 1981. Saturn’s rings - Azimuthal variations, phase curves, and radial profiles in four colors. *Icarus*, **46**, 187–200.
- Thomson, F. S., Marouf, E. A., Tyler, G. L., French, R. G., and Rappoport, N. J. 2007. Periodic microstructure in Saturn’s rings A and B. *GeoRL*, **34**, L24203.
- Tiscareno, M. S. 2013. A modified Type I migration model for propeller moons in Saturn’s rings. *PSS*, **77**(Mar.), 136–142.
- Tiscareno, M. S., Burns, J. A., Nicholson, P. D., Hedman, M. M., and Porco, C. C. 2007. Cassini imaging of Saturn’s rings. II. A wavelet technique for analysis of density waves and other radial structure in the rings. *Icarus*, **189**, 14–34.
- Toomre, A. 1964. On the gravitational stability of a disk of stars. *ApJ*, **139**(May), 1217–1238.
- Tremaine, S. 2003. On the Origin of Irregular Structure in Saturn’s Rings. *AJ*, **125**, 894–901.
- Ulrich, M.-H. 2000. The active galaxy NGC 4151: Archetype or exception? *AARv*, **10**, 135–178.
- van Lieshout, R., Min, M., and Dominik, C. 2014. Dusty tails of evaporating exoplanets. I. Constraints on the dust composition. *A&A*, **572**, A76.
- Varnière, P., and Tagger, M. 2006. Reviving Dead Zones in accretion disks by Rossby vortices at their boundaries. *A&A*, **446**, L13–L16.
- Verbiscer, A. J., Skrutskie, M. F., and Hamilton, D. P. 2009. Saturn’s largest ring. *Nature*, **461**, 1098–1100.
- Villaver, E., and Livio, M. 2007. Can Planets Survive Stellar Evolution? *ApJ*, **661**, 1192–1201.
- Volonteri, M. 2010. Formation of supermassive black holes. *AARv*, **18**, 279–315.
- Wada, K., Tanaka, H., Suyama, T., Kimura, H., and Yamamoto, T. 2008. Numerical Simulation of Dust Aggregate Collisions. II. Compression and Disruption of Three-Dimensional Aggregates in Head-on Collisions. *ApJ*, **677**, 1296–1308.
- Wada, K., Tanaka, H., Okuzumi, S., Kobayashi, H., Suyama, T., Kimura, H., and Yamamoto, T. 2013. Growth efficiency



- of dust aggregates through collisions with high mass ratios. *A&A*, **559**, A62.
- Wagoner, R. V. 1999. Relativistic diskoseismology. *PhR*, **311**, 259–269.
- Ward, W. R. 1981. On the radial structure of Saturn’s rings. *GeoRL*, **8**, 641–643.
- Ward, W. R. 1997. Protoplanet Migration by Nebula Tides. *Icarus*, **126**(Apr.), 261–281.
- Wardle, M. 1999. The Balbus-Hawley instability in weakly ionized discs. *MNRAS*, **307**, 849–856.
- Warner, B. 1995. Cataclysmic variable stars. *Cambridge Astrophysics Series*, **28**.
- Warner, B., and Nather, R. E. 1971. Observations of rapid blue variables - II. U Geminorum. *MNRAS*, **152**, 219–229.
- Weidenschilling, S. J. 1977. Aerodynamics of solid bodies in the solar nebula. *MNRAS*, **180**, 57–70.
- Weidenschilling, S. J., Chapman, C. R., Davis, D. R., and Greenberg, R. 1984. Ring particles - Collisional interactions and physical nature. Pages 367–415 of: Greenberg, R., and Brahic, A. (eds), *IAU Colloq. 75: Planetary Rings*.
- Weidenschilling, S. J., Spaute, D., Davis, D. R., Marzari, F., and Ohtsuki, K. 1997. Accretional Evolution of a Planetary Swarm. *Icarus*, **128**, 429–455.
- Wetherill, G. W., and Stewart, G. R. 1989. Accumulation of a swarm of small planetesimals. *Icarus*, **77**, 330–357.
- Wetherill, G. W., and Stewart, G. R. 1993. Formation of planetary embryos - Effects of fragmentation, low relative velocity, and independent variation of eccentricity and inclination. *Icarus*, **106**, 190.
- Williams, J. P., and Cieza, L. A. 2011. Protoplanetary Disks and Their Evolution. *ARAA*, **49**, 67–117.
- Windmark, F., Birnstiel, T., Güttler, C., Blum, J., Dullemond, C. P., and Henning, T. 2012. Planetary formation by sweep-up: how the bouncing barrier can be beneficial to growth. *A&A*, **540**, A73.
- Wisdom, J., and Tremaine, S. 1988. Local simulations of planetary rings. *AJ*, **95**, 925–940.
- Wurm, G., Paraskov, G., and Krauss, O. 2005. Growth of planetesimals by impacts at 25 m/s. *Icarus*, **178**, 253–263.
- Wyatt, M. C. 2003. Resonant Trapping of Planetesimals by Planet Migration: Debris Disk Clumps and Vega’s Similarity to the Solar System. *ApJ*, **598**, 1321–1340.
- Wyatt, M. C. 2005a. Spiral structure when setting up pericentre glow: possible giant planets at hundreds of AU in the HD 141569 disk. *A&A*, **440**, 937–948.
- Wyatt, M. C. 2005b. The insignificance of P-R drag in detectable extrasolar planetesimal belts. *A&A*, **433**, 1007–1012.
- Wyatt, M. C. 2008. Evolution of Debris Disks. *ARAA*, **46**, 339–383.
- Wyatt, M. C., and Dent, W. R. F. 2002. Collisional processes in extrasolar planetesimal discs - dust clumps in Fomalhaut’s debris disc. *MNRAS*, **334**, 589–607.
- Wyatt, M. C., Panić, O., Kennedy, G. M., and Matrà, L. 2015. Five steps in the evolution from protoplanetary to debris disk. *ApSS*, **357**, 103.
- Xiang-Gruess, M. 2016. Generation of highly inclined protoplanetary discs through single stellar flybys. *MNRAS*, **455**(Jan.), 3086–3100.
- Xu, S., Jura, M., Koester, D., Klein, B., and Zuckerman, B. 2014. Elemental Compositions of Two Extrasolar Rocky Planetesimals. *ApJ*, **783**, 79.
- Youdin, A. N., and Goodman, J. 2005. Streaming Instabilities in Protoplanetary Disks. *ApJ*, **620**, 459–469.
- Zhang, K., Blake, G. A., and Bergin, E. A. 2015. Evidence of Fast Pebble Growth Near Condensation Fronts in the HL Tau Protoplanetary Disk. *ApJL*, **806**, L7.
- Zuckerman, B., Koester, D., Reid, I. N., and Hüensch, M. 2003. Metal Lines in DA White Dwarfs. *ApJ*, **596**, 477–495.